Electronic Effects in C-H and C-C Bond Activation: State-Specific Reactions of $Fe^+(^6D,^4F)$ with Methane, Ethane, and Propane

Richard H. Schultz,[†] J. L. Elkind,[‡] and P. B. Armentrout*[†,⊥]

Contribution from the Department of Chemistry, University of California, Berkeley, California 94720. *Received July 3, 1987*

Abstract: Reactions of atomic iron ions with methane, ethane, and propane are studied with guided ion beam mass spectrometry. By using different ion sources, different electronic states of the ion can be prepared and studied in detail. The first excited state, $Fe^+(^4F)$, is more reactive than the ground state, $Fe^+(^6D)$, for all endothermic reactions in all three systems. This result is similar to recent observations of the reactions of these states with H_2. The different reactivities are explained by using simple molecular orbital arguments. In contrast, $Fe^+(^4F)$ reacts *less* efficiently than $Fe^+(^6D)$ in the exothermic reactions of ethane and propane below 0.5 eV but more efficiently at higher energies. This behavior is explained by a potential energy surface crossing that is avoided at low kinetic energies due to spin-orbit interactions and is permitted at higher energies. Finally, analysis of the threshold behavior of the endothermic reactions provides the bond dissociation energies, $D°(Fe^+-CH_3) = 2.51 \pm 0.10$ eV (57.9 ± 2.4 kcal/mol) and $D°(FeH) = 1.98 \pm 0.13$ eV (45.7 ± 3.0 kcal/mol).

Recent advances in our laboratory have enabled us to examine state-specific reactions of atomic transition-metal ions. One of the most interesting of these studies found that the ^6D ground state of Fe^+ is more than an order of magnitude less reactive with molecular hydrogen than the first excited state, $Fe^+(^4F)$, even though it is only 0.25 eV lower in energy.[1] A natural question to consider is whether the strong state dependence observed in reactions of transition-metal ions with dihydrogen also occurs in reactions with alkanes. Are the same ideas used to understand H-H bond activation useful in describing gas-phase C-H and C-C bond activation? We might expect similarities since these reactions all involve activation of covalent σ bonds. On the other hand, as the neutral molecule gets larger, it has more internal degrees of freedom. This might allow relaxation of strict symmetry rules and thus alter the relative reactivities of different electronic states. A related issue stems from the observation that in the condensed phase, C-C bond activation is much more difficult than C-H bond activation,[2] while gas-phase ions activate both with facility. Is this difference due to some intrinsic difference in the electronic requirements for C-H versus C-C activation or is it due to differences in the gas-phase versus condensed-phase metal center? The present study was undertaken with the goal of examining these issues for the reactions of Fe^+ with small alkanes.

The reactions of Fe^+ with alkanes have been studied previously with ion cyclotron resonance (ICR) mass spectroscopy,[3] Fourier transform mass spectroscopy (FTICR),[4,5] flowing afterglow,[6] and ion beam techniques.[7] Since Fe^+ reacts exothermically and efficiently only with alkanes larger than ethane, ion beam techniques are required to investigate the reactions of Fe^+ with methane and ethane and the endothermic channels of reactions with larger alkanes. Beauchamp and co-workers have performed ion beam studies of Fe^+ and alkanes although with no state selectivity.[7] Both ICR and beam studies generally conclude that reaction with the larger alkanes proceeds via insertion of Fe^+ into a C-H or C-C bond. The present study reexamines both the beam and ICR results and the conclusions drawn from them in light of the state specific data acquired here.

Experimental Section

Experiments are performed on a guided ion beam apparatus, a detailed description of which has been presented elsewhere.[8] Ions are extracted from the source (described below), accelerated, and focused into a magnetic sector for mass analysis. The present study uses the ^{56}Fe isotope (91.66% natural abundance). The mass selected ion beam is decelerated to the desired interaction energy and focused into an octopole ion trap.

Table I. Electronic States of Fe^+ below 2.5 eV

state	config	E (eV)[a]	population[b]
^6D	$4s3d^6$	0.052	0.783 ± 0.011
^4F	$3d^7$	0.300	0.213 ± 0.009
^4D	$4s3d^6$	1.032	0.004 ± 0.001
^4P	$3d^7$	1.688	<0.001
^2G	$3d^7$	1.993	
^2P	$3d^7$	2.298	

[a] Statistical average over all J levels. Energies taken from the following: Corliss, C.; Sugar, J. *J. Phys. Chem. Ref. Data* **1982**, *11*, 135-241. [b] Maxwell-Boltzmann distribution at 2300 ± 100 K.

This device uses radio frequency electric fields to trap ions in the radial direction and ensure collection of all ionic products and transmitted reactant ions. The octopole passes through a collision chamber into which the reactant gas is admitted. To ensure that single-collision conditions are maintained, the reactant gas is held at low pressures, typically 0.03 to 0.08 mTorr, as measured by an MKS Baratron capacitance manometer. The product ions and unreacted beam are extracted from the octopole, focused into a quadrupole mass filter for mass analysis, and detected with use of a scintillation ion counter and standard ion counting techniques. Reaction conditions and data collection are controlled by a DEC MINC computer. Raw ion intensities are converted to absolute reaction cross sections as described previously.[8] Absolute cross sections are estimated to have uncertainties of ±20%. Relative uncertainties are within ±5% for cross sections in excess of σ(min), which depends on the source (see below) and is limited by statistical counting uncertainties for smaller cross sections.

The absolute energy of the ions in the interaction region is determined by using the octopole as a retarding field analyzer. Because the retarding and interaction regions are physically the same, this energy measurement has minimal uncertainties caused by space charge, contact potentials, and focusing aberrations. The reliability of this energy measurement has been verified by time-of-flight measurements[8] and by comparison with theoretical cross sections.[9] The energy scale has an uncertainty of ~0.05 eV lab, which is equivalent to 0.01 eV CM for reactions of Fe^+ with CH_4

[†] Present address: Chemistry Department, University of Utah, Salt Lake City, UT 84112.
[‡] Chemistry Department, Rice University, Houston, TX 77251.
[⊥] NSF Presidential Young Investigator 1984-1989; Alfred P. Sloan Fellow.

(1) Elkind, J. L.; Armentrout, P. B. *J. Am. Chem. Soc.* **1986**, *108*, 2765-2767; *J. Phys. Chem.* **1986**, *90*, 5736-5745.
(2) Crabtree, R. H. *Chem. Rev.* **1985**, *85*, 245-269.
(3) Byrd, G. D.; Burnier, R. C.; Freiser, B. S. *J. Am. Chem. Soc.* **1982**, *104*, 3365-3369.
(4) (a) Allison, J.; Freas, R. B.; Ridge, D. P. *J. Am. Chem. Soc.* **1979**, *101*, 1332-1333. (b) Freas, R. B.; Ridge, D. P. *Ibid.* **1980**, *102*, 7129-7131. (c) Larsen, B. S.; Ridge, D. P. *Ibid.* **1984**, *106*, 1912-1922.
(5) Jacobson, D. B.; Freiser, B. S. *J. Am. Chem. Soc.* **1983**, *105*, 5197-5206.
(6) Tonkyn, R.; Weisshaar, J. C. *J. Phys. Chem.* **1986**, *90*, 2305-2308; *Ibid.*, submitted for publication.
(7) (a) Armentrout, P. B.; Halle, L. F.; Beauchamp, J. L. *J. Am. Chem. Soc.* **1981**, *103*, 6501-6502. (b) Halle, L. F.; Armentrout, P. B.; Beauchamp, J. L. *Organometallics* **1982**, *1*, 963-968. (c) Houriet, R.; Halle, L. F.; Beauchamp, J. L. *Ibid.* **1983**, *2*, 1818-1829.
(8) Ervin, K. M.; Armentrout, P. B. *J. Chem. Phys.* **1985**, *83*, 166-189.
(9) Burley, J. D.; Ervin, K. M.; Armentrout, P. B. *Int. J. Mass Spectrom. Ion Proc.*, in press.

0002-7863/88/1510-0411$01.50/0

Table II. Literature Thermochemistry in kcal/mol[a]

species	$\Delta H_f°_{298}$	species	$\Delta H_f°_{298}$
Fe	99.3 ± 0.3	C_2H_6	−20.0 ± 0.1[b]
Fe^+	282.3 ± 1.8	C_3H_5	39.4 ± 1.5[d]
H	52.1	C_3H_6	4.8 ± 0.2[b]
H^-	33.2	1-C_3H_7	22.6 ± 1.1[e]
CH_2	92.3 ± 1.0	1-$C_3H_7^+$	212.0 ± 1.2[f]
CH_3	34.8 ± 0.2	2-C_3H_7	20.0 ± 1.1[e]
CH_4	−17.9 ± 0.1	2-$C_3H_7^+$	191.2 ± 1.2[f]
C_2H_4	12.5 ± 0.1[b]	C_3H_8	−25.0 ± 0.1[b]
C_2H_5	28.3 ± 1.1[c]		

[a] All values, except where noted, are from the following: Chase, M. W., et al. *J. Phys. Chem. Ref. Data* **1985**, *14*, Suppl. No. 1. [b] Pedley, J. B.; Naylor, R. D.; Kirby, S. P. *Thermochemical Data of Organic Compounds*; Chapman and Hall: London, 1986. [c] Doering, W. v. E. *Proc. Natl. Acad. Sci. U.S.A.* **1981**, *78*, 5279–5283. [d] Baulch, D. L.; Cox, R. A.; Hampson, R. F., Jr.; Kerr, J. A.; Troe, J.; Watson, R. T. *J. Phys. Chem. Ref. Data* **1984**, *13*, 1259–1378. [e] Marshall, R. M.; Rahman, L. *Int. J. Chem. Kinet.* **1977**, *9*, 705. [f] Schultz, J. C.; Houle, F. A.; Beauchamp, J. L. *J. Am. Chem. Soc.* **1984**, *106*, 3917–3927. These values have been increased by 1.48 kcal/mol to conform to the ion convention that includes the enthalpy of the electron.

and 0.02 eV CM for reactions with C_2H_6 and C_3H_8.

Ions are produced in two ways. Surface ionization (SI) is used to produce a beam containing a known distribution of excited state ions. In the SI source, $Fe(CO)_5$ is passed through a water-cooled inlet line into an evacuated source chamber and over a rhenium filament that is resistively heated to 2300 ± 100 K, as measured by optical pyrometry. Dissociation of the $Fe(CO)_5$ and ionization of the resultant iron atoms occurs on the filament. If the ions reach equilibrium at the filament temperature, this method should produce a beam with a Maxwell–Boltzmann distribution of states (Table I). Previous studies in our lab indicate that this is a reasonable approximation.[1,10-13] To produce a pure beam of ground-state ions, a drift cell source (DC) is used. Here, Fe^+ ions, produced by electron impact ionization of $Fe(CO)_5$ at an electron energy of ~100 eV, are passed through a drift cell that contains a bath of Ar gas, typically at 250 mTorr. A field of 1 to 2 V/cm pulls the ions across the drift cell. As described in earlier papers,[1,12] the ~1000 collisions that an ion undergoes as it crosses the drift cell are sufficient to relax nearly all excited ions to the ground state. To ensure that the Fe^+ ions are in the ground state in each experiment performed here, we verified that reaction with D_2 yields similar results to those observed for the ground state in our previous study.[1] For the SI source, σ(min) is $\sim 10^{-18}$ cm^2. For the DC source, σ(min) is higher, $\sim 10^{-17}$ cm^2, due to the less intense ion beams produced by this source relative to the SI source. $Fe(CO)_5$ (99.5%) is obtained from Alfa and used without further purification except for multiple freeze–pump–thaw cycles.

A full description of the mathematical modeling of cross sections for reactions like process 1 is given in earlier papers.[10,11,14] Exothermic

$$Fe^+ + BC \rightarrow FeB^+ + C - \Delta E \quad (1)$$

reaction channels are often modeled by the Langevin–Gioumousis–Stevenson (LGS)[15] form of the cross section, eq 2, where e is the unit of electric charge, α is the polarizability of the neutral molecule, and E is

$$\sigma_{LGS} = \pi e(2\alpha/E)^{1/2} \quad (2)$$

the relative translational energy of the reactants. Endothermic channels are more useful for more directly determining the thermodynamics of a system. Assuming no activation barrier in excess of the reaction endothermicity, ΔE, an accurate measurement of the reaction threshold yields the value of the bond strength of Fe^+–B, $D°(Fe^+–B) = D°(BC) - \Delta E$, since the bond strength of BC is generally known. Theory and experiment both show that excitation functions in the threshold region can be modeled by eq 3,[10,11,14,16] where σ_0 is an energy-independent scaling

$$\sigma(E) = \sigma_0(E - \Delta E)^n/E^m \quad (3)$$

Table III. Best Fit Parameters for Fitting Routine[a]

ionic product	neutral reactant		m = 0.0	1.0	1.5	3.0	n
FeH^+	CH_4	n =	0.6	0.7	0.8	1.1	0.8
		ΔE =	2.10	2.10	2.10	2.10	2.08
	C_2H_6	n =	1.3	1.7	1.9	2.5	2.1
		ΔE =	1.93	1.88	1.86	1.80	1.84
	C_3H_8	n =	1.5	1.9	2.2	2.9	2.8
		ΔE =	2.29	2.23	2.20	2.11	2.12
$FeCH_3^+$	C_2H_6	n =	1.2	1.8	2.1	3.1	3.3
		ΔE =	1.22	1.15	1.11	1.02	1.00
	C_3H_8	n =	1.3	2.0	2.3	3.4	4.8
		ΔE =	1.18	1.08	1.04	0.94	0.85
$FeC_2H_5^+$	C_3H_8	n =	1.5	2.0	2.2	3.2	3.4
		ΔE =	1.36	1.31	1.29	1.21	1.18
$C_3H_7^+$	C_3H_8	n =	1.3	1.7	1.9	2.6	2.2
		ΔE =	1.93	1.89	1.87	1.79	1.83

[a] All energies in eV.

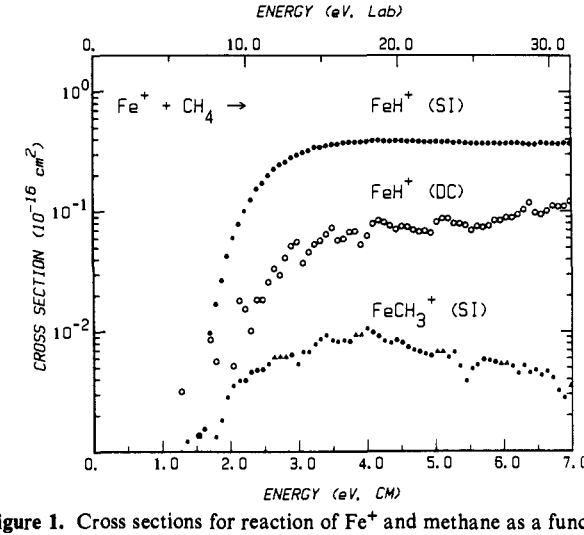

Figure 1. Cross sections for reaction of Fe^+ and methane as a function of kinetic energy in the center-of-mass frame (lower scale) and laboratory frame (upper scale). Closed and open symbols are results for Fe^+ produced in the SI and DC sources, respectively.

factor, E is the total energy available to the reactants, ΔE is the reaction endothermicity, and n and m are parameters that depend on the theoretical model being used. In this study, this equation is evaluated for the cases where m = 0, 1, 1.5, 3, and n for each reaction channel. The parameters n, σ_0, and ΔE are allowed to vary freely to best fit the data. This comparison is made after the theoretical cross sections are convoluted over the known experimental energy distribution of the ion beam and Doppler broadening due to random thermal motion of the neutral reactant gas.[8] The ΔE determined for a particular reaction is fairly insensitive to the values of n and m used (Table III). The line-of-centers model ($n = m = 1$), which we have used extensively to analyze the data for reactions of atomic metal ions with dihydrogen,[11,17] cannot reproduce the data for reactions of Fe^+ with larger neutral species such as those studied here. A similar conclusion was drawn in an earlier study of reactions of vanadium ions with ethane.[10a]

At higher energies, the cross sections peak and then fall off. This behavior can have two causes. The cross section for production of FeB^+ can decrease if another product channel, such as process 4, becomes thermodynamically allowed and competes favorably with formation of

$$Fe^+ + BC \rightarrow FeC^+ + B \quad (4)$$

FeB^+. Such coupling implies that the two products, FeB^+ and FeC^+, share the same precursor intermediate and helps establish the mechanism of the reaction. The cross section for FeB^+ can also decrease when the

(10) (a) Aristov, N.; Armentrout, P. B. *J. Am. Chem. Soc.* **1986**, *108*, 1806–1819. (b) Aristov, N.; Armentrout, P. B. *Ibid.*, in press.
(11) (a) Elkind, J. L.; Armentrout, P. B. *J. Phys. Chem.* **1985**, *89*, 5626–5636. (b) Elkind, J. L.; Armentrout, P. B. *Ibid.* **1986**, *90*, 6576–6586. (c) Elkind, J. L.; Armentrout, P. B. *J. Chem. Phys.* **1986**, *84*, 4862–4871.
(12) Elkind, J. L.; Armentrout, P. B. *J. Phys. Chem.* **1987**, *91*, 2037–2045.
(13) Sunderlin, L. S.; Armentrout, P. B. *J. Phys. Chem.*, in press.
(14) Georgiadis, R.; Armentrout, P. B. *J. Am. Chem. Soc.* **1986**, *108*, 2119–2126.
(15) Gioumousis, G.; Stevenson, D. P. *J. Chem. Phys.* **1958**, *29*, 294.
(16) Levine, R. D.; Bernstein, R. B. *Molecular Reaction Dynamics*; Oxford University Press: New York, 1974; Chapter 2.
(17) Elkind, J. L.; Armentrout, P. B. *J. Chem. Phys.* **1987**, *86*, 1868–1877.
(18) Hanratty, M. A.; Beauchamp, J. L.; Illies, A. J.; Bowers, M. T. *J. Am. Chem. Soc.* **1985**, *107*, 1788–1789. Hanratty, M. A.; Beauchamp, J. L.; Illies, A. J.; van Koppen, P.; Bowers, M. T. *Ibid.*, submitted for publication.
(19) Georgiadis, R.; Schultz, R. H.; Armentrout, P. B., work in progress.
(20) The observed ratio of $FeCH_3^+$:$FeCD_3^+$ is 5:4. A similar effect was also observed in the reaction of Sc^+ with CH_3CD_3 (ref 22). There simple angular momentum arguments were outlined which suggest that $FeCH_3^+$ should be favored by a 8:7 ratio.

amount of internal energy available to the product ion exceeds the energy necessary to fragment the molecule. The overall process, reaction 5, has

$$Fe^+ + BC \rightarrow FeB^+ + C \rightarrow Fe^+ + B + C \quad (5)$$

a thermodynamic threshold at $D°(BC)$. Simple cleavage reactions are often observed to peak near $D°(BC)$.

Results

Fe^+ + Methane. Two ionic products are observed for the reaction of Fe^+(SI) and methane: FeH^+ (process 6) and $FeCH_3^+$ (process 7). These are shown in Figure 1. Despite a careful

$$Fe^+ + CH_4 \rightarrow FeH^+ + CH_3 \quad (6)$$

$$\rightarrow FeCH_3^+ + H \quad (7)$$

search, no other products could be seen for the reaction of Fe^+(SI) and CH_4. Both reaction 6 and reaction 7 have comparable apparent thresholds of ~1.5 eV yet the $FeCH_3^+$ cross section is smaller than that of FeH^+ by a factor of about 40. Although Halle, Armentrout, and Beauchamp (HAB) did not report absolute reaction cross sections in their investigation of the reactions of Fe^+(SI) and small alkanes,[7b] they also noted a similar large difference in cross sections for reactions 6 and 7.

Above ~4 eV, $\sigma(FeH^+)$ remains roughly constant while σ-$(FeCH_3^+)$ begins to decline. In contrast, when FeH^+ is produced by reaction of Fe^+(SI) with H_2, its cross section decreases rapidly above 4.5 eV, $D°(H_2)$. Since the thermodynamic threshold for dissociation of both FeH^+ and $FeCH_3^+$ occurs at $D°(H_3C–H)$ = 4.5 eV, the observed behavior implies that the methyl radical product in reaction 6 carries away much more of the excess available energy, either in internal modes or in translation, than a hydrogen atom. For reaction 7, $\sigma(FeCH_3^+)$ declines beginning at about $D°(CH_3–H)$ since the neutral hydrogen atom product can carry away little energy.

The reactivity of Fe^+(DC) with methane is much less than that of Fe^+(SI) (Figure 1). No new channels are observed. The maximum FeH^+ cross section is lowered by a facor of about 4, while $\sigma(FeCH_3^+)$ is below our limit of detectability, ~0.03 Å^2. As discussed in an earlier report,[1] Fe^+(DC) is believed to consist almost entirely of ground-state $Fe^+(^6D)$ while Fe^+(SI) contains ~20% of the ^4F first excited state (Table I). Thus the differences in reactivity between Fe^+(SI) and Fe^+(DC) reflect a larger reactivity for $Fe^+(^4F)$. The conversion of the raw DC and SI data to the true state behavior is straightforward. At 2300 ± 100 K, the SI beam contains 78.3 ± 1.0% $Fe^+(^6D)$ and 21.3 ± 1.0% $Fe^+(^4F)$. To extrapolate to the true behavior of the $Fe^+(^4F)$ excited state, the DC data (scaled by a factor of 0.783) are subtracted from the SI data and the remainder divided by 0.213.

The results of such a calculation for the FeH^+ product are shown in Figure 2. They show that $Fe^+(^6D)$ is considerably less reactive with methane than $Fe^+(^4F)$. The peak cross section of the ground-state data for reaction 6 is only 0.1 Å^2 and occurs at >7 eV, well above $D°(H_3C–H)$ = 4.5 eV. Reaction by the first excited state, on the other hand, reaches a maximum cross section of 1.6 Å^2 at about 4 eV. This behavior is comparable to that observed with $Fe^+ + H_2$ where the maximum cross sections are 0.15 Å^2 at 7 eV and 2.2 Å^2 at 4 eV for $Fe^+(^6D)$ and $Fe^+(^4F)$, respectively.[1] For the $FeCH_3^+$ product, the true cross section for the ^6D state is unknown and therefore the maximum ^4F state cross section is 0.05 Å^2, i.e., 4.7 (=1/0.213) times the SI cross section shown in Figure 1.

Fe^+ + Ethane. In reaction of Fe^+(SI) with ethane, two major channels are observed, reactions 8 and 9, and two minor channels, reactions 10 and 11, as shown in Figure 3. $\sigma(FeH^+)$ again does

$$Fe^+ + C_2H_6 \rightarrow FeH^+ + C_2H_5 \quad (8)$$

$$\rightarrow FeCH_3^+ + CH_3 \quad (9)$$

$$\rightarrow FeC_2H_5^+ + H \quad (10)$$

$$\rightarrow FeC_2H_4^+ + H_2 \quad (11)$$

not decline appreciably above $D°(C_2H_5–H)$ = 4.35 eV (Table II). In contrast, $\sigma(FeCH_3^+)$ has a broad peak near $D°(H_3C–CH_3)$ = 3.9 eV and begins to decline above about 4.5 eV. These observations are in good accord with the qualitative observations of HAB, who were only able to detect reactions with cross sections in excess of 0.03 Å^2, i.e., processes 8 and 9.[7b]

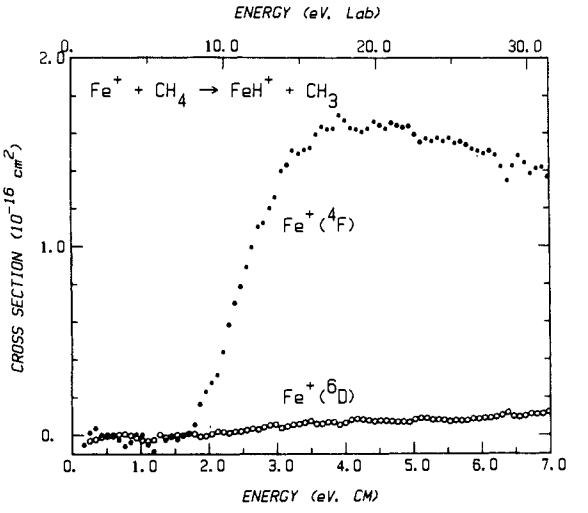

Figure 2. State-specific cross sections for reaction 6 as a function of kinetic energy in the center-of-mass frame (lower scale) and laboratory frame (upper scale). Closed and open symbols are results for $Fe^+(^4F)$ and $Fe^+(^6D)$, respectively, as derived from the data in Figure 1; see text.

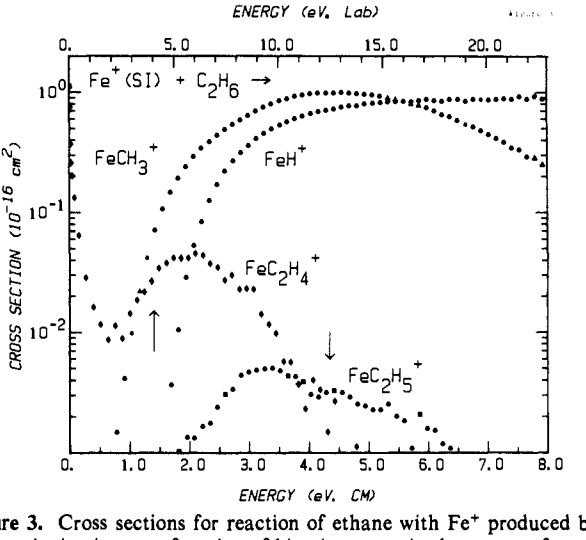

Figure 3. Cross sections for reaction of ethane with Fe^+ produced by surface ionization as a function of kinetic energy in the center-of-mass frame (lower scale) and laboratory frame (upper scale). Arrows indicate the energy needed to dehydrogenate ethane, 1.4 eV, and the C–H bond energy, 4.35 eV.

Several researchers[3,4c,7b] have previously commented on their inability to see process 11, the dehydrogenation of ethane by Fe^+. As can be seen in Figure 3, this reaction does occur, although very inefficiently. The cross section appears to have two distinct parts. At energies below 0.4 eV, there is an exothermic reaction that has an efficiency of about 1/500 of LGS (eq 2) at 0.1 eV but which declines as $E^{-1.1\pm0.3}$. There is also an apparently endothermic feature that has an onset of 0.2–0.5 eV and peaks at 2.1 ± 0.1 eV. The position of this peak correlates very well with the onset of reaction 8 (Figure 3), which may imply that the decline in $\sigma(FeC_2H_4^+)$ is due to competition from reaction 8. This behavior is unexpected since the thermodynamic threshold for dissociation of $FeC_2H_4^+$ formed in reaction 11 into $Fe^+ + C_2H_4$ is only 1.4 eV. Since $\sigma(FeC_2H_4^+)$ continues to rise for another 0.7 eV, we can deduce that a significant amount of energy is put into kinetic or perhaps internal excitation of the products. This is consistent with observations by Hanratty et al.[18] that dehydrogenation of alkanes by Co^+ and Ni^+ exhibits substantial kinetic energy release.

As with methane, reaction of ethane with Fe^+(DC) yields strikingly different results from reaction with Fe^+(SI) (Figure

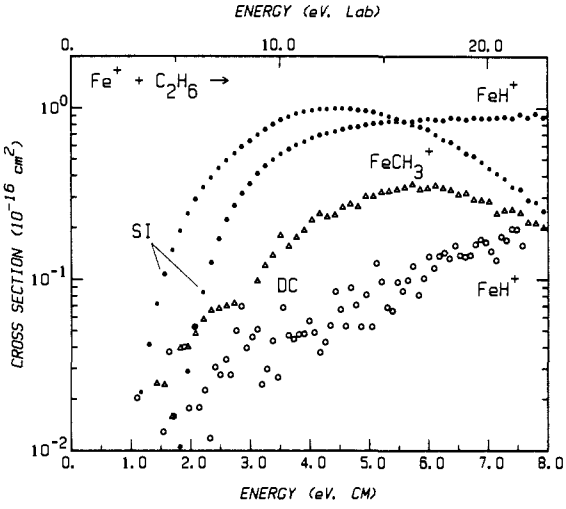

Figure 4. Cross sections for reactions 8 (circles) and 9 (triangles) as a function of kinetic energy in the center-of-mass frame (lower scale) and laboratory frame (upper scale). Closed and open symbols are results for Fe^+ produced in the SI and DC sources, respectively.

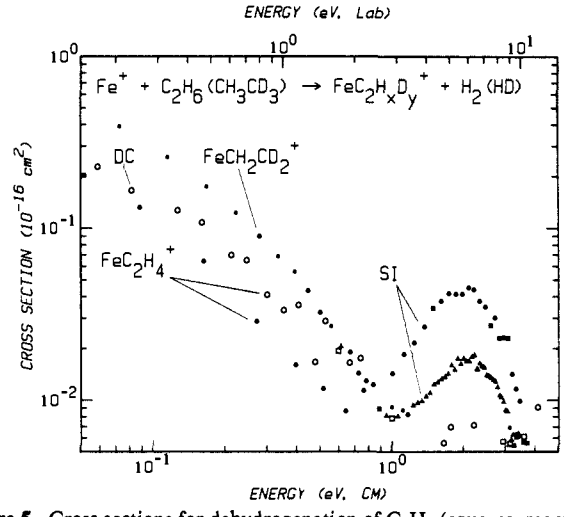

Figure 5. Cross sections for dehydrogenation of C_2H_6 (squares, reaction 11) and CH_3CD_3 (triangles) by Fe^+ as a function of kinetic energy in the center-of-mass (lower scale) and laboratory (upper scale) frames. Closed and open symbols are results for Fe^+ produced in the SI and DC sources, respectively.

4). The cross sections of all four processes are decreased. $\sigma(FeH^+)$ rises very slowly such that it reaches a maximum at >8 eV. At this energy, it is about one-fifth the maximum FeH^+ cross section from Fe^+(SI). The qualitative behavior of reaction 9 is similar, although the quantitative change is less. The peak in $\sigma(FeCH_3^+)$ is shifted from about 4 eV to about 5.7 eV, and the maximum cross section is half. For Fe^+(DC), process 10 is below our detectability limit.

The most intriguing observation concerns the behavior of process 11. For reaction of Fe^+(DC), the exothermic part of the cross section remains, but the endothermic feature disappears (Figure 5). We performed several experiments to determine the exact nature of the exothermic portion of reaction 11 since exothermic dehydrogenation of C_2H_6 by Fe^+ has not been previously reported. In particular, we endeavored to determine if the highly inefficient exothermic portion of the cross section might be due to the presence of small numbers of highly excited Fe^+ ions. One piece of evidence against this hypothesis is the recurrence of this feature with roughly the same cross section for ions produced in the DC source (Figure 5). Since Fe^+(DC) is almost entirely ground state, the size of the exothermic tail should decrease if it were due to the more highly excited states which constitute <0.5% of the SI beam (Table I). Additional experiments verify that the signal at the $FeC_2H_4^+$ mass is not due to impurities either in the ethane

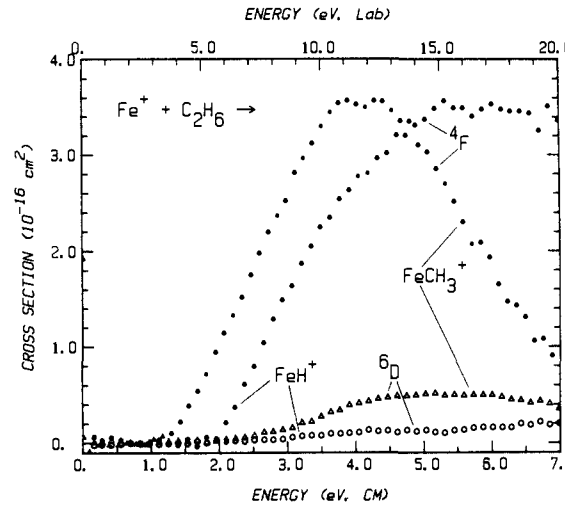

Figure 6. State-specific cross sections for reactions 8 (circles) and 9 (triangles) as a function of kinetic energy in the center-of-mass (lower scale) and laboratory (upper scale) frames. Closed and open symbols are results for $Fe^+(^4F)$ and $Fe^+(^6D)$, respectively, as derived from the data in Figure 4; see text.

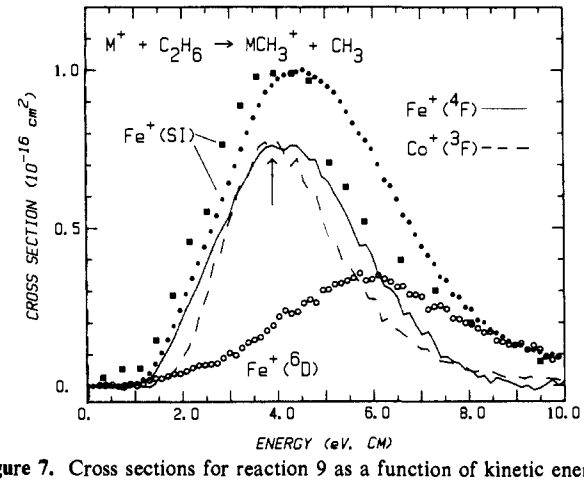

Figure 7. Cross sections for reaction 9 as a function of kinetic energy in the center-of-mass frame (lower scale). Closed circles show results for Fe^+ produced in the SI source (same data as Figures 3 and 4). Squares show results from HAB, ref 7b, obtained under similar conditions and scaled to the present data. Open circles show results for Fe^+ produced in the DC source, $Fe^+(^6D)$, reduced by a factor of 0.78. The difference between this data and the SI data is shown as a solid line and is the reactivity due to $Fe^+(^4F)$, uncorrected for its population. For comparison, the dashed line shows the cross section for the analogous reaction of $Co^+(^3F)$, ref 19, scaled to the $Fe^+(^4F)$ cross section. The arrow indicates the C–C bond energy at 3.9 eV.

or in the vacuum chamber. Also, the analogous reaction of Fe^+ with CH_3CD_3 to yield $FeC_2H_2D_2^+$ and HD has an exothermic portion with a comparable cross section to that of reaction 11 (Figure 5). We therefore conclude that $Fe^+(^6D)$ does exothermically dehydrogenate ethane, although very inefficiently.

State-specific results for reactions 8 and 9 are shown in Figure 6. The cross section for reaction 10 presumably behaves similarly although this cannot be determined with certainty. Clearly, $Fe^+(^4F)$ is still considerably more reactive than the $Fe^+(^6D)$ ground state in the endothermic reactions of $Fe^+ + C_2H_6$. The exothermic component of reaction 11, however, is due primarily to $Fe^+(^6D)$.

Our ability to resolve the Fe^+(SI) reactivity into that for the individual ionic states enables us to explain some apparently anomalous observations by HAB.[7b] In their study of the reactions of Fe^+(SI) and ethane, they noted that $\sigma(FeCH_3^+)$ falls off slowly compared to analogous reactions of Co^+ and Ni^+. Further, the absolute magnitude of the $FeCH_3^+$ cross section was smaller than the $CoCH_3^+$ and $NiCH_3^+$ cross sections despite the fact that the Fe^+ reaction is less endothermic. As shown in Figure 7, the slow decline of the Fe^+(SI) data is due to contributions from the

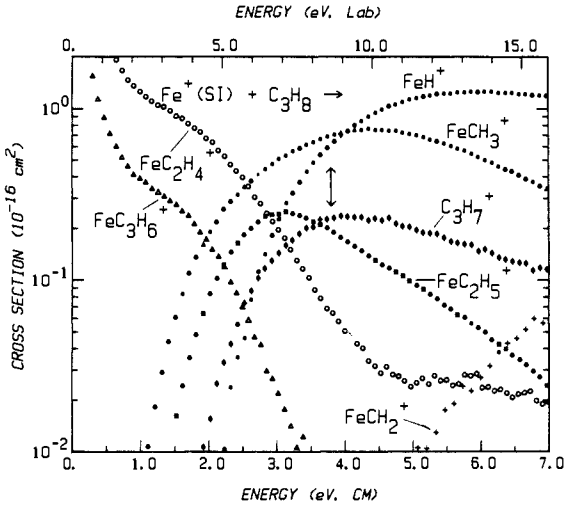

Figure 8. Cross sections for reaction of propane with Fe^+ produced in the surface ionization source as a function of kinetic energy in the center-of-mass frame (lower scale) and laboratory frame (upper scale). The arrow indicates the C–C bond energy at 3.8 eV.

reaction of $Fe^+(^6D)$. The overall shape of the $Fe^+(^4F,3d^7)$ cross section is similar to those observed for the ground electronic states of $Co^+(^3F,3d^8)$ and $Ni^+(^2D,3d^9)$[7b,19] (Figure 7) but is somewhat broader. Also the absolute magnitude of the $Fe^+(^4F)$ cross section, $\sigma(\max) \approx 3.6$ Å^2 (Figure 6), now exceeds those for Co^+ and Ni^+, both $\sigma(\max) \approx 2$ Å^2. Similar observations have been made for the reactions of $Fe^+(^4F)$, $Co^+(^3F)$, and $Ni^+(^2D)$ with dihydrogen and shown there to be a consequence of the relative thermodynamics of these systems.[12]

Fe^+ + Ethane-*1,1,1-d*$_3$. In the reactions of Fe^+(SI) with CH_3CD_3, analogous processes to reactions 8–11 are seen. FeD^+ and FeH^+ are produced in approximately equal amounts, each with a peak cross section of about half that of reaction 8. Both $FeCH_3^+$ and $FeCD_3^+$ are produced in nearly equal amounts,[20] with cross sections about half those of process 9. No mixed isotopic species ($FeCH_2D^+$ or $FeCHD_2^+$) are observed. The analogue to reaction 10 produces both $FeC_2H_3D_2^+$ and $FeC_2H_2D_3^+$ in equal amounts. Loss of molecular hydrogen yields only the 1,2-dehydrogenation product, $FeCH_2CD_2^+$, for both the exothermic and endothermic parts of the reaction, indicating that the ionic product of process 11 is an iron–ethylene ion and that no scrambling is occurring. The cross section for dehydrogenation in this system (Figure 5) is similar to that for process 11 in shape and magnitude although there are systematic differences.

Fe^+ + Propane: Endothermic Reactions. The major products of the reaction of Fe^+(SI) and propane are shown in Figure 8. We observe four primary endothermic channels, reactions 12–15. For reactions 12 and 13, which compete directly, $\sigma(C_3H_7^+)$ has

$$Fe^+ + C_3H_8 \rightarrow FeH^+ + C_3H_7 \quad (12)$$

$$\rightarrow C_3H_7^+ + FeH \quad (13)$$

$$\rightarrow FeCH_3^+ + C_2H_5 \quad (14)$$

$$\rightarrow FeC_2H_5^+ + CH_3 \quad (15)$$

a lower threshold than $\sigma(FeH^+)$ but a smaller maximum. While our apparatus cannot detect neutral species directly, reaction 16 cannot occur until 4.2 eV (Table II). Therefore, $C_3H_7^+$ formation

$$Fe^+ + C_3H_8 \rightarrow C_3H_7^+ + Fe + H \quad (16)$$

at threshold must be due to reaction 13.

The cross sections for formation of iron methyl and iron ethyl ions in reactions 14 and 15 are comparable in magnitude and energy dependence to that for the analogous C–C bond activation process observed with ethane (reaction 9). $\sigma(FeCH_3^+)$ peaks at 4.35 ± 0.15 eV, somewhat above the C–C bond energy of 3.8 eV. As with reaction 9, this late peak is due to the presence of $Fe^+(^6D)$ in the SI beam. $\sigma(FeC_2H_5^+)$, however, peaks at 3.1 ± 0.1 eV, which is much lower than the C–C bond strength. It is possible that this early decline is due to competition from process 14, but the threshold behavior shows no obvious effects of such competition. Also, $\sigma(FeC_2H_5^+)$ produced in reaction 10 peaks at about the same energy as process 15 does (Figure 3), but well below the ethane C–H bond energy of 4.35 eV. In this system, the competitive channel, formation of FeH^+, has a much larger cross section than $\sigma(FeC_2H_5^+)$ and a different energy behavior than reaction 14. A more likely explanation for the early peak in both systems is that $FeC_2H_5^+$ decomposes into $FeH^+ + C_2H_4$ or perhaps $FeC_2H_4^+ + H$ rather than into $Fe^+ + C_2H_5$. This hypothesis is consistent with the known thermochemistry. For $FeC_2H_5^+$ formed in reaction 15, dissociation by loss of ethene has a thermodynamic threshold of 3.25 ± 0.06 eV, based on $D°(Fe^+–H) = 2.16 \pm 0.06$ eV.[1] The threshold for H atom loss cannot be determined reliably since $D°(Fe^+–C_2H_4)$ is not well established, but it must be less than 4.0 eV (see discussion below). Experimentally, formation of FeH^+ via this route cannot be observed since FeH^+ is formed much more efficiently via reaction 12; however, formation of $FeC_2H_4^+$ via this route can be seen as the cross section at high energies (Figure 8). Since the size of this cross section cannot account for all of the decline in $\sigma(FeC_2H_5^+)$, this species presumably decomposes primarily to $FeH^+ + C_2H_4$.

At higher energies, we also observe formation of $FeCH_2^+$ (Figure 8), which could be formed in reactions 17a, 17b, or 17c. Unfortunately, detailed analysis of the threshold for this product

$$Fe^+ + C_3H_8 \rightarrow FeCH_2^+ + C_2H_6 \quad (17a)$$

$$\rightarrow FeCH_2^+ + C_2H_4 + H_2 \quad (17b)$$

$$\rightarrow FeCH_2^+ + C_2H_5 + H \quad (17c)$$

is complicated by the small size of its cross section and the possibility of incomplete mass resolution from the much more intense $FeCH_3^+$ cross section. However, from the value of the $FeCH_2^+$ bond of 3.56 ± 0.22 eV[21] and thermochemistry from Table II, we can calculate that the endothermicities of reaction 17a, 17b, and 17c are 0.66 ± 0.22, 2.07 ± 0.22, and 5.02 ± 0.22 eV, respectively. The largest feature in the $FeCH_2^+$ cross section has an apparent threshold of approximately 5 eV. We attribute this to reaction 17c and infer that it is a minor decomposition channel of $FeCH_3^+$. A very small contribution to the cross section begins at about 2 eV. This may arise from reaction 17b but it is also possible that it is due to mass overlap from the $FeCH_3^+$ cross section, which has a similar energy dependence. This feature could also be due to reaction 17a if an appreciable activation barrier (~1.4 eV) is present; a barrier of 0.6 to 0.9 eV is present for the analogous process in the reaction of Sc^+ with ethane.[22]

At energies above 3 eV, we see several minor endothermic products of the reaction of Fe^+(SI) and propane: $FeCH^+$, $FeC_2H_2^+$, $FeC_2H_3^+$, $FeC_3H_3^+$, and $FeC_3H_5^+$. The peak cross section for $FeCH^+$ is 0.015 Å^2 at ~10 eV and that for $FeC_2H_3^+$ is 0.01 Å^2 at 5.5 eV. The peak cross sections for the remaining products are all less than 0.005 Å^2. With the exception of the $FeC_3H_5^+$ product, these products do not appear until energies above 4 eV. This observation and the small sizes of their cross sections imply that they arise from decomposition of primary ionic products. The $FeC_3H_5^+$ product has the lowest threshold of these minor products, 2 and 3 eV, and could be produced via reaction 18a or 18b. Despite a careful search, $FeC_3H_7^+$ was not observed.

$$Fe^+ + C_3H_8 \rightarrow \begin{cases} FeC_3H_7^+ + H & (18a) \\ FeC_3H_6^+ + H_2 & (18b) \end{cases} \rightarrow FeC_3H_5^+ + H_2 + H$$

It is possible that any $FeC_3H_7^+$ which is formed rapidly dehydrogenates to form $FeC_3H_5^+$ (reaction 18a). Analogous behavior has been postulated for all Co^+–alkyl species having 3 or more carbons.[23] Dehydrogenation of $FeC_3H_7^+$ may actually be exo-

(21) Hettich, R. L.; Freiser, B. S. *J. Am. Chem. Soc.* **1984**, *106*, 2537–2540. Hettich, R. L.; Jackson, T. C.; Stanko, E. M.; Freiser, B. S. *J. Am. Chem. Soc.* **1986**, *108*, 5086–5093.

(22) Sunderlin, L. S.; Aristov, N.; Armentrout, P. B. *J. Am. Chem. Soc.* **1987**, *109*, 78–89.

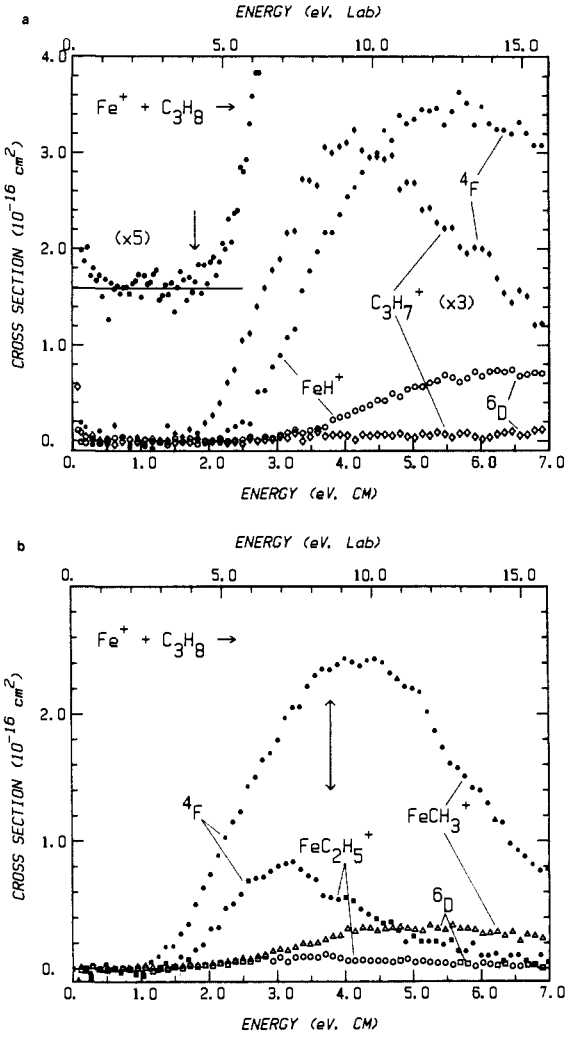

Figure 9. State-specific cross sections for endothermic reactions of Fe^+ with propane as a function of kinetic energy in the center-of-mass frame (lower scale) and laboratory frame (upper scale). Closed and open symbols are results for $Fe^+(^4F)$ and $Fe^+(^6D)$, respectively, derived as discussed in the text. Part a shows results for reactions 12 (circles) and 13 (diamonds, scaled up by a factor of 3). The inset shows the cross section for FeH^+ scaled up by a factor of 5 and offset from zero. The arrow indicates the approximate thermodynamic threshold at 1.8 eV. Part b shows results for reactions 14 (triangles) and 15 (squares). The arrow indicates the C–C bond energy of 3.8 eV.

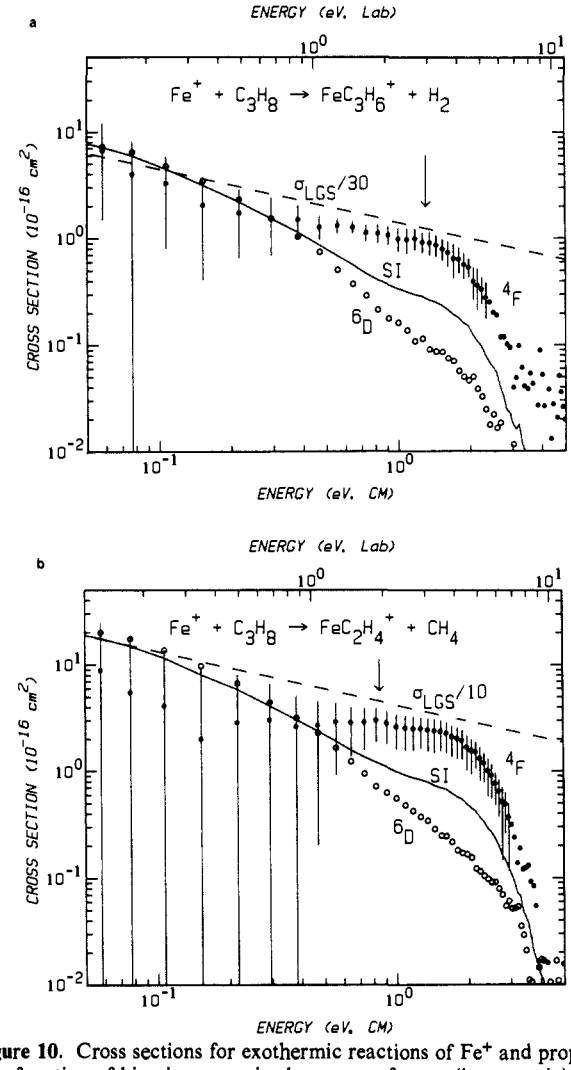

Figure 10. Cross sections for exothermic reactions of Fe^+ and propane as a function of kinetic energy in the center-of-mass (lower scale) and laboratory (upper scale) frames. Part a shows results for reaction 19 and part b shows results for reaction 20. Closed and open symbols show results for $Fe^+(^4F)$ and $Fe^+(^6D)$ (equivalent to DC data), respectively, derived as discussed in the text. Solid lines show results for Fe^+ produced in the surface ionization (SI) source. Dashed lines show σ_{LGS} (eq 2) divided by 30 (part a) and 10 (part b). Vertical bars show one standard deviation uncertainties in the derived cross sections for reaction of $Fe^+(^4F)$. Arrows indicate the thresholds for reaction 21 at 1.3 eV (part a) and reaction 22 at 0.85 eV (part b).

thermic since the allyl ligand could bind more strongly to the metal ion than C_3H_7 and dehydrogenation of free C_3H_7 requires only ~0.8 eV (Table II).

Endothermic reactions of Fe^+(DC) and propane behave similarly to those of Fe^+(DC) in the other systems studied. The DC cross sections reach maxima that are smaller than those of the corresponding SI cross sections by factors of 3 to 5, and they occur at higher kinetic energies. Figure 9 shows the results for reactions 12–15 resolved into state-specific cross sections. The difference in reactivities is roughly the same magnitude as that seen with ethane.

Fe^+ + Propane: Exothermic Reactions. We observe two exothermic products in the reaction of Fe^+(SI) and propane: dehydrogenation to $FeC_3H_6^+$ (reaction 19) and demethanation to $FeC_2H_4^+$ (reaction 20). This is consistent with all previous

$$Fe^+ + C_3H_8 \rightarrow FeC_3H_6^+ + H_2 \quad (19)$$

$$\rightarrow FeC_2H_4^+ + CH_4 \quad (20)$$

results.[3,4c,5,7] Their cross sections are shown in Figure 8 and in more detail for both sources in Figure 10. Their cross sections increase with decreasing energy as low in energy as we can measure (<0.05 eV), showing that these reactions proceed without an activation barrier. At energies below 0.2 eV, $\sigma(FeC_3H_6^+)$ and $\sigma(FeC_2H_4^+)$ are about 3% and 10% of the collision limit (eq 2), respectively. Both cross sections decline as $E^{-1.0\pm0.2}$ below 2 eV and as $E^{-3.7\pm0.9}$ above.

We measure a constant branching ratio of 75 ± 4% $FeC_2H_4^+$ and 25 ± 4% $FeC_3H_6^+$ for reaction energies below 1.5 eV. This ratio has previously been measured at thermal energies by Freiser and co-workers as 70/30 by FTICR[5] and 76/24 by ICR[3] and by Weisshaar and co-workers as 70/30 in a flowing afterglow.[6] Beauchamp and co-workers derived branching ratios from their ion beam studies of 56/44 at ~1 eV[7b] and 82/18 at ~0.5 eV.[7c] We observe the branching ratio to increase in favor of the $FeC_2H_4^+$ product above 1.5 eV until it reaches 94/6 at ~4 eV. Above this energy, $\sigma(FeC_3H_6^+)$ is too small to make a quantitative comparison with $\sigma(FeC_2H_4^+)$. The ratio changes because the $FeC_3H_6^+$ product decomposes at lower energies than the $FeC_2H_4^+$ product. This is unexpected because the most likely decomposition pathways for the $FeC_3H_6^+$ and $FeC_2H_4^+$ products are reaction 21 which

(23) Armentrout, P. B.; Beauchamp, J. L. *J. Am. Chem. Soc.* **1981**, *103*, 784–791.

(24) Formation of $Fe^+{=}CHCH_2CH_3$ is estimated to be higher in energy than Fe^+–propene by about 2.2 eV by assuming that $D°(Fe^+{=}CHCH_2CH_3) \approx D°(Fe^+{=}CH_2)$.

can begin at 1.29 eV and reaction 22 which can begin at a *lower*

$$Fe^+ + C_3H_8 \rightarrow Fe^+ + C_3H_6 + H_2 \quad (21)$$

$$\rightarrow Fe^+ + C_2H_4 + CH_4 \quad (22)$$

energy of 0.85 eV (Table II). Instead, the sharp decline in $\sigma(FeC_3H_6^+)$ and $\sigma(FeC_2H_4^+)$ at high energies may be due to competition from the endothermic channels (reactions 12–15; Figure 8). The failure of the cross sections to fall off at the thresholds for reactions 21 and 22 indicates that significant energy must be released into translation or internal energy of the neutral product. Once again, these results are similar to those of Hanratty et al., who showed that dehydrogenation of alkanes by Co^+ and Ni^+ exhibit substantial kinetic energy release.[18] However, these workers find that when Co^+ and Ni^+ induce the loss of small alkanes, analogous to reaction 20, the kinetic energy release is statistical and peaks near zero. The discrepancy between these findings and the present results could be due to differences between Fe^+ and these other metals or it may indicate that the CH_4 species lost in reaction 20 carries away considerable energy in internal modes (something which H_2 cannot do easily). The latter is the more probable explanation since, as we shall see, the cross sections for $Fe^+(^4F)$ have the same high-energy behavior as $Fe^+(SI)$ and this state is expected to have comparable reactivity to the ground states for Co^+ and Ni^+.

For $Fe^+(DC)$, the exothermic channels exhibit a much different type of behavior relative to $Fe^+(SI)$ than do the endothermic channels (Figure 10). Now the DC data are comparable in size to the SI data below 0.5 eV, clearly indicating that $Fe^+(^6D)$ is reactive at low energy in these channels. The branching ratio, 76 ± 2% $FeC_2H_4^+$ to 24 ± 2% $FeC_3H_6^+$, is identical with that seen with SI. Comparison of several sets of SI and DC data shows that they have similar shapes below 0.5 eV and that the SI data has a magnitude that is 0.85 ± 0.17 times that of the DC data. If $Fe^+(^4F)$ were completely unreactive at low energy, the magnitude of the SI data would be 0.78 times that of the DC data. Conversion of this data into state-specific cross sections (Figure 10) is again straightforward although the subtraction of two large cross sections results in a $Fe^+(^4F)$ cross section with a large absolute uncertainty. For instance, it can be shown that below 0.3 eV, $\sigma(^4F)/\sigma(^6D) \approx 0.33 \pm 0.80$. Thus, at the lowest energies, $Fe^+(^6D)$ is at least as reactive as and in all likelihood is *more* reactive than $Fe^+(^4F)$. Above 0.5 eV, this relative reactivity reverses to return to the effect seen in the endothermic channels.

Fe^+ + Propane-*2,2-d*$_2$. Experiments with $Fe^+(SI)$ and $CH_3CD_2CH_3$ establish the site of hydride abstraction from propane. Both FeH^+ and FeD^+ are observed with a ratio of close to three to one, the ratio of primary-to-secondary positions. In contrast, $C_3H_6D^+$ is observed but $C_3H_5D_2^+$ is not. Clearly, hydride abstraction (reaction 13) occurs only at the 2-position such that FeD and a 2-propyl ion, $C_3H_6D^+$, are formed. Thus, the homolytic bond cleavage of C–H bonds in propane by Fe^+ to form FeH^+ is random with no site preference, while heterolytic C–H bond cleavage to form FeH (FeD) is highly selective. This difference in selectivity is easily rationalized. The homolytic bond strengths of the 1-position and 2-position C–H bonds differ by only 0.11 eV (Table II). On the other hand, the heterolytic bond strengths at the 1- and 2-positions differ by 0.90 eV due primarily to the large difference in ionization potentials of 1-C_3H_7 (8.15 eV) and 2-C_3H_7 (7.36 eV) (Table II). This study marks the first explicit observation of such behavior for a metal ion reaction.

In the analogues of reactions 14 and 15, we observe the products expected from simple C–C bond cleavage ($FeCH_3^+$ and $FeCD_2CH_3^+$). No scrambling appears to be occurring in these endothermic reactions. For the analogue to reaction 19, the primary dehydrogenation product is 1,2 dehydrogenation to form $FeC_3H_5D^+$ + HD. 1,3 or 1,1 dehydrogenation to form $FeC_3H_4D_2^+$ + H_2 is also seen, with a cross section approximately one-fifth the size independent of energy below 1 eV. 2,2 dehydrogenation to produce $FeC_3H_6^+$ + D_2 has no more than three percent of the cross section for 1,2 dehydrogenation. Random dehydrogenation would yield loss of 53% H_2, 43% HD, and 4% D_2 compared to the 16%, 81%, and <3% seen here. If the occurrence of both H_2 and HD loss were due to isotope scrambling in a long-lived intermediate, we would expect the branching ratio to depend on energy. Since it does not below 1 eV, we conclude that 1,2 dehydrogenation is the dominant pathway for loss of hydrogen with contributions from 1,3 dehydrogenation. Exothermic 1,1 dehydrogenation to form Fe^+–propylidene can probably be eliminated on the basis of thermochemistry.[24] Houriet et al. also concluded that hydrogen scrambling was negligible in reactions of Fe^+ with alkanes.[7c] For the analogue to reaction 20, demethanation occurs primarily to yield $FeC_2H_2D_2^+$ + CH_4. The two other possible demethanation product channels, $FeC_2H_3D^+$ + CH_3D and $FeC_2H_4^+$ + CH_2D_2, have no more than 5% the cross section of the primary isotopic product.

Thermochemistry

Cross sections for the various endothermic products can be analyzed by using eq 3 as described above to yield thermodynamic data for these species. The results of these analyses are summarized in Table III. In all cases, data for $Fe^+(SI)$ are analyzed. On the basis of the comparison of the state-specific cross sections, these thresholds correspond to reaction of $Fe^+(^4F)$ in all cases. The electronic energy of this state, E_{el}, must therefore be included when converting these thresholds to thermochemical values of interest, i.e., $D°(Fe^+–B) = D°(BC) - \Delta E - E_{el}$. At 2300 K, the average energy of the ^4F state is 0.284 eV. No analysis is attempted for the $Fe^+(DC)$ data because these cross sections are small and rise slowly from threshold making accurate analysis difficult. The final values of ΔE reported below are averages of all 5 fits given in Table III. Uncertainties are determined from the spread in these values and the absolute uncertainty in the energy scale. All derived thermodynamic quantities are presumed to be at 298 K. No corrections for the internal energies of the neutral reagents are made.[10a]

Fe^+–H. The thresholds for reactions 6 and 8 are 2.10 ± 0.02 and 1.86 ± 0.06 eV, respectively. Using $D°(H_3C–H) = 4.54 \pm 0.01$ eV and $D°(H–C_2H_5) = 4.35 \pm 0.05$ eV calculated from Table II and correcting for E_{el}, we derive Fe^+–H bond energies at 298 K of 2.16 ± 0.03 and 2.21 ± 0.08 eV from the results of reactions 6 and 8, respectively. These values are consistent with and help confirm the value derived from the reaction of Fe^+ and H_2, 2.16 ± 0.06 eV (49.8 ± 1.4 kcal/mol).[1]

In the propane system, the observed threshold for reaction 12, 2.19 ± 0.08 eV, yields an anomalously low Fe^+–H bond energy of 1.74 ± 0.10 eV if $D°(2\text{-}C_3H_7–H) = 4.21 \pm 0.05$ eV is used. Even if $D°(1\text{-}C_3H_7–H) = 4.32 \pm 0.05$ eV is used, the bond energy derived, 1.85 ± 0.10 eV, is still inconsistent with all other values. Clearly, the threshold measured in the propane system is not the thermodynamic threshold of ~1.8 eV. The most likely explanation for such behavior is a kinetic shift due to competition from reaction 19. Such competition would cause the cross section for reaction 12 to rise slowly from the true threshold, such that the apparent threshold is too high. In fact, a close examination of the data for reaction 12 in the threshold region (Figure 9) reveals that the initial rise in the cross section could begin as low as 1.8 eV.

We have pointed out previously[14] that our modeling procedure can yield bond energies that are systematically too low in cases where the cross section rises slowly from the thermodynamic threshold. The example discussed here shows that such systematic errors can usually be identified by comparison of bond strengths derived from several different systems. When the bond strengths are consistent from system to system (as is generally the case), we can infer that the reactions have neither activation barriers nor kinetic shifts.

Fe–H. In its reaction with propane, $Fe^+(^4F)$ abstracts H^- to form neutral FeH in process 13. By using the observed threshold of 1.86 ± 0.06 eV from Table III, $D°(2\text{-}C_3H_7^+–H^-) = 10.81 \pm 0.06$ eV from Table II, and E_{el}, we derive a heterolytic bond strength for $D°(Fe^+–H^-)$ of 8.67 ± 0.09 eV. This value is related to the homolytic bond strength for $D°(Fe–H)$ by eq 23, where the ionization potential (IP) of Fe is 7.87 ± 0.06 eV and the

$$D°(Fe–H) = D°(Fe^+–H^-) - IP(Fe) + EA(H) \quad (23)$$

electron affinity (EA) of H is 0.76 ± 0.02 eV (Table II). The resulting value of $D°$(Fe–H) is 1.56 ± 0.11 eV (36.0 ± 2.5 kcal/mol). This value is of questionable accuracy, however, because it is likely that the true threshold is not observed for reaction 13 for the same reason that the true threshold of reaction 12 is obscured, namely, the direct competition of reactions 12 and 13 with one another and probably with reaction 19 as well. Therefore, the value derived is strictly a *lower* limit to the true bond energy. More detailed inspection of the threshold region again reveals that the cross section rises slowly from an apparent threshold below 1.86 eV.

Another approach to obtaining the thermochemistry for FeH assumes that the difference in thresholds for reactions 12 and 13 is a valid measure of the relative ionization potentials of FeH and 2-C_3H_7. Our observed difference in the analyzed thresholds (Table III) is 0.33 ± 0.10 eV. Since the IP of 2-C_3H_7 is 7.36 ± 0.02 eV (Table II), this assumption implies that IP(FeH) = 7.69 ± 0.10 eV. The homolytic bond strength is given by eq 24 such that $D°$(FeH) = 1.98 ± 0.13 eV (45.7 ± 3.0 kcal/mol) and

$$D°(\mathrm{FeH}) = D°(\mathrm{Fe^+–H}) + \mathrm{IP(FeH)} - \mathrm{IP(Fe)} \quad (24)$$

$D°(Fe^+–H^-)$ = 9.09 ± 0.13 eV (eq 23). We believe these values to be more accurate than those derived above.

Other experimental determinations of the FeH bond strength span a number of techniques. Dendramis et al.[25] performed a Birge–Sponer analysis on the Fe–H stretching frequency observed for FeH trapped in an argon matrix at 4 K. They derived a value of 2.0 eV, but corrected this to 1.7 eV since bond strengths derived from Birge–Sponer extrapolations are generally about 20% too high. Kant and Moon[26] determined an upper limit for $D°$(FeH) of 1.86 eV using a mass spectrometric/third law method; however, this value was calculated by incorrectly assuming that the ground state of FeH is $^6\Sigma$. Sallans et al.[27] determined the bond strength of FeH by observing exothermic proton-transfer reactions between Fe^- and various acids. Their derived bond strength of 1.30 ± 0.13 eV is thus a lower limit. Tolbert and Beauchamp[28] used a similar bracketing technique with Fe^+ and hydride donors to get a value of 1.78 ± 0.13 eV < $D°$(FeH) < 2.09 ± 0.13 eV. The present determination of the Fe–H bond energy is consistent with the spectroscopic, mass spectrometric, and hydride transfer results within error limits. The result from proton transfer studies appears to be accurate only as a lower limit.

FeH has also been the subject of considerable theoretical study. The first calculations of the FeH bond strength were done by Das[29] and Walch and Bauschlicher[30] for the $^6\Delta$ state of FeH. More recent experimental data have shown that the ground state of FeH is in fact $^4\Delta$ with the $^6\Delta$ state 0.25 eV higher in energy.[31] Correcting the calculated values for this $^4\Delta$–$^6\Delta$ splitting yields values of 1.60 and 2.08 eV, respectively. More recent theoretical calculations by Krauss and Stevens[32] and Chong et al.[33] yield values for the FeH bond energy of 1.47 and 1.55 eV. Chong et al. also comment that the $^4\Delta$ state of FeH is the first-row transition-metal hydride least amenable to theoretical analysis. Clearly, these theoretical calculations are not yet accurate enough to provide a basis for definitively choosing among the various experimental values.

Fe^+–CH_3. We can derive a value for the iron methyl ion bond energy from reactions 9 and 14 in the ethane and propane systems. The data for the methane system (reaction 7) are too scattered to provide a reliable Fe^+–CH_3 bond strength. The thresholds for reactions 9 and 14 are 1.10 ± 0.12 and 1.02 ± 0.16 eV, respectively. Using $D°(H_3C–CH_3)$ = 3.89 ± 0.01 eV and $D°(C_2H_5–CH_3)$ = 3.82 ± 0.05 eV, and correcting for E_{el}, we derive values of 2.51 ± 0.12 and 2.52 ± 0.17 eV for $D°(Fe^+–CH_3)$ from the two systems. Our best determination for this bond energy is the average of these values, 2.51 ± 0.10 eV (57.9 ± 2.4 kcal/mol).

HAB derived a value for the Fe^+–CH_3 bond of 3.0 ± 0.2 eV from their observed threshold of 0.91 eV for the reaction of Fe^+(SI) + ethane (process 9).[7b] Correcting this value for the presence of $Fe^+(^4F)$ yields a bond strength of 2.7 ± 0.2 eV, in agreement with the present value within experimental error. Freiser and co-workers[21] recently used photodissociation to obtain a Fe^+–CH_3 bond strength of ≤2.82 ± 0.22 eV. This value is an upper limit since the true photodissociation threshold may not be observed.

The bond strength of Fe^+–CH_3 is 0.35 ± 0.13 eV (8 ± 3 kcal/mol) greater than that of Fe^+–H. This contrasts with results for solution-phase species where metal–hydrogen bonds are generally stronger than metal–carbon bonds.[34] The most common suggestion for this disparity has been that the bare gas-phase metal ion has no steric constraints in forming either of these bonds. Since H and CH_3 are isolobal ligands, they should be expected to form similar bonds of similar strength.[23,34–36] The gas-phase metal–CH_3 bond can be stronger than the metal–H bond because the methyl group is more polarizable than a hydrogen atom, and hence the positive ion attracts it more strongly.[23,37]

Fe^+–C_2H_4. As discussed above, we believe the exothermic portion of reaction 11 to be a true representation of the behavior of the $Fe^+(^6D)$ + ethane system. Since this reaction is exothermic, the Fe^+–C_2H_4 bond strength must exceed the energy needed to dehydrogenate ethane (1.41 eV, Table II). Also, C_2D_4 is known to displace CO from $FeCO^+$,[38] which means that $D°(Fe^+–C_2H_4) > D°(Fe^+–CO)$. Photoionization (PI) experiments[39] find that $D°(Fe^+–CO)$ = 2.62 ± 0.1 eV, but this value has been questioned by HAB, who suggest that the PI data are consistent with a bond energy as low as 1.63 eV.[7b] This is supported by photodissociation measurements, $D°(Fe^+–CO) \leq 1.9$ eV[40] and $D°(Fe^+–C_2H_4) \leq 1.7$ eV.[41]

Other transition-metal–ethene bond strengths are $D°(Sc^+–C_2H_4) > 1.52$ eV;[22] $D°(V^+–C_2H_4) \approx 2.2$ eV;[10a] $D°(Co^+–C_2H_4)$ = 2.0 ± 0.4 eV;[18] and $D°(Ni^+–C_2D_4) > 2.1 \pm 0.2$ eV.[42] As a first approximation, it might be expected that the binding energy of ethene to Fe^+ should be comparable to that for Co^+ and Ni^+, ~2.1 eV. However, this comparison needs to be made between similar electronic states, namely ground-state $Co^+(^3F,3d^8)$ and $Ni^+(^2D,3d^9)$, and excited state $Fe^+(^4F,3d^7)$. This implies that $D°[Fe^+(^4F)–C_2H_4] \approx 2.1 \pm 0.4$ eV and $D°[Fe^+(^6D)–C_2H_4] \approx 1.8 \pm 0.4$ eV (42 ± 9 kcal/mol), in agreement with the results above.

The Fe^+(SI) data for reaction 11 exhibit an apparently endothermic feature. This feature cannot be due to the loss of two H atoms rather than H_2, since such a reaction would imply that $D°(Fe^+–C_2H_4) > 4.9$ eV, a value clearly inconsistent with prior literature values. The origins of this unusual feature will be discussed in more detail below.

Fe^+–C_2H_5. Analysis of the threshold of reaction 15 in order

(25) Dendramis, R. J.; Van Zee, R. J.; Weltner, W., Jr. *Astrophys. J.* **1979**, *231*, 632–636.
(26) Kant, A.; Moon, K. A. *High Temp. Sci.* **1981**, *14*, 23–31.
(27) Sallans, L.; Lane, K. R.; Squires, R. R.; Freiser, B. S. *J. Am. Chem. Soc.* **1985**, *107*, 4379–4385.
(28) Tolbert, M. A.; Beauchamp, J. L. *J. Phys. Chem.* **1986**, *90*, 5015–5022.
(29) Das, G. *J. Chem. Phys.* **1981**, *74*, 5766–5774.
(30) Walch, S. P.; Bauschlicher, C. W., Jr. *J. Chem. Phys.* **1983**, *78*, 4597–4605.
(31) Mead, R. D.; Stevens, A. E.; Lineberger, W. C. In *Gas Phase Ion Chemistry*; Bowers, M. T., Ed.; Academic: New York, 1984; Vol. III.
(32) Krauss, M.; Stevens, W. J. *J. Chem. Phys.* **1985**, *82*, 5584.
(33) Chong, D. P.; Langhoff, S. R.; Bauschlicher, C. W., Jr.; Walch, S. P.; Partridge, H. *J. Chem. Phys.* **1986**, *85*, 2850–2860. The value is calculated from $D_5°$(Fe–H) = 1.67 eV by using their value of ω_e, 1915 cm^{-1}, and correcting from 0 to 298 K.
(34) Halpern, J. *Inorg. Chim. Acta* **1985**, *100*, 41–48.
(35) Saillard, J.-Y.; Hoffmann. R. *J. Am. Chem. Soc.* **1984**, *106*, 2006–2026.
(36) Schilling, J. B.; Goddard, W. A.; Beauchamp, J. L. *J. Am. Chem. Soc.* **1987**, *109*, 5573–5580.
(37) Mandich, M. L.; Halle, L. F.; Beauchamp, J. L. *J. Am. Chem. Soc.* **1984**, *106*, 4403–4411.
(38) Foster, M. S.; Beauchamp, J. L. *J. Am. Chem. Soc.* **1975**, *97*, 4808.
(39) Distefano, G. *J. Res. Natl. Bur. Stand., Sect. A* **1970**, *74A*, 233.
(40) Cassady, D. J.; Freiser, B. S. *J. Am. Chem. Soc.* **1984**, *106*, 6176.
(41) Freiser, B. S. *Talanta* **1985**, *32*, 697–708.
(42) Halle, L. F.; Houriet, R.; Kappes, M. M.; Staley, R. H.; Beauchamp, J. L. *J. Am. Chem. Soc.* **1982**, *104*, 6293–6297.

to determine the iron ethyl ion bond strength is complicated by overlap from reaction 20. Because of incomplete mass resolution of the two channels, the data for reaction 15 contain an exothermic tail that is ~2% of the cross section for reaction 20 and parallels it closely. The true cross section for reaction 15 is obtained by subtracting out this contribution although this procedure results in scattered data in the threshold region. Analysis of this $FeC_2H_5^+$ cross section yields a threshold of 1.27 ± 0.09 eV, which leads to a Fe^+–C_2H_5 bond energy of 2.27 ± 0.11 eV. While this is 0.24 ± 0.16 eV weaker than the Fe^+–CH_3 bond energy, the value determined here is insufficiently precise to tell whether this difference is significant. Also, this comparison may not be meaningful if the ground-state structure of $FeC_2H_5^+$ is not a metal–ethyl ion (I) but rather the hydrido–metal–ethene ion (II). If so, the derived thermochemistry indicates that the HFe^+–ethene bond strength is 1.66 ± 0.13 eV. This value is consistent with the Fe^+–ethene

$$\underset{\text{I}}{Fe^+—C_2H_5} \qquad \underset{\text{II}}{H—Fe^+—\|}$$

bond energy determined above. Therefore the thermochemical data do not unambiguously distinguish between I and II as the preferred ground-state structure of $FeC_2H_5^+$. As noted in the Results, this ion appears to decompose by loss of C_2H_4, which may imply structure II, although this evidence is also not unambiguous. Halle et al.[43] observe that FeH^+ reacts exothermically with C_2D_4 to form FeD^+, which shows that rearrangement of I and II is possible when $FeC_2H_5^+$ has enough internal energy to decompose to FeH^+ + C_2H_4, and that II decomposes primarily by loss of ethene.

Reaction Mechanisms

Fe^+ + Dihydrogen. In addition to the thermochemistry discussed above, we can also deduce information about the mechanisms of reaction and the potential energy surfaces (PESs) on which the reactions occur. A useful starting point for this discussion is our results for the reactions of dihydrogen with Fe^+ and other atomic transition-metal ions. These reactions can be understood by using molecular orbital (MO) arguments that have been detailed elsewhere.[11,12,17] These arguments contend that the difference in reactivity of $Fe^+(^6D)$ and $Fe^+(^4F)$ is due to the electron configurations of these states, $4s3d^6$ and $3d^7$, respectively. Since the 4s is the largest orbital on the metal ion, it is the first to interact with H_2. In C_{2v} symmetry, the 4s mixes with the $\sigma_g(H_2)$ orbital to form bonding and antibonding orbitals of a_1 symmetry. Since the $\sigma_g(H_2)$ orbital is doubly occupied, the bonding a_1 MO is always doubly occupied. If the 4s is occupied (as for $Fe^+(^6D)$), the antibonding a_1* is occupied leading to a repulsive interaction. This is relieved somewhat by interaction in $C_{\infty v}$ symmetry, but repulsive interactions between the 3d electrons and the H_2 make deviations from collinear geometries unfavorable for $Fe^+(^6D)$. As a consequence, the reaction of the ground state is inefficient, rises slowly from threshold, and reaches a maximum at high energies. This type of behavior is characteristic of an impulsive process where two-body interactions dominate.[11c]

If the 4s orbital is empty (as for $Fe^+(^4F)$), these repulsive interactions are avoided. Further, the empty $\sigma_u(H_2)$ orbital interacts with a doubly occupied $3d\pi$ orbital to form a second bonding–antibonding pair of MOs with b_2 symmetry. Only the bonding b_2 MO is occupied such that this interaction is attractive and can lead to a dihydride intermediate. However, the $3d^7$ configuration means that the $3d\sigma$ orbital is occupied. Since this orbital has the same symmetry as the 4s, it can also lead to repulsive interactions in C_{2v} symmetry. While not expected to be as severe as the repulsion from 4s occupation, this interaction can apparently prevent formation of a statistically behaved intermediate at the elevated energies necessary to drive the reaction. Consequently, $Fe^+(^4F)$ reacts via an efficient, direct mechanism. While this reaction does not appear to involve a long-lived, statistically behaved intermediate, its cross section rises from the thermodynamic threshold and reaches a maximum at the H_2 bond energy. These observations show that extensive three-body interactions do occur for $Fe^+(^4F)$.

Fe + Alkanes: Thermochemical Estimates and Potential Energy Surfaces. The conclusion that neither state of Fe^+ reacts by inserting into the H_2 molecule contrasts with the generally accepted[3-5,7,23] mechanism for the reactions of Fe^+ with alkanes: insertion into C–H and C–C bonds followed by β-H or β-alkyl transfer and reductive elimination of dihydrogen or an alkane, Scheme I (R = H or CH_3). Before discussing the individual alkane systems studied, it is useful to consider the thermodynamic and electronic characteristics of these proposed intermediates and the resultant PESs. Unfortunately, the amount of quantitative information available for these systems is still meager. We therefore explore what is known and what assumptions might be useful.

One pertinent experimental result is the observation that Fe^+ exothermically decarbonylates acetone, which implies $D°[Fe^+–2(CH_3)] > 96$ kcal/mol, or $D°(H_3CFe^+–CH_3) > 38 \pm 3$ kcal/mol.[44] This result is somewhat ambiguous, however, since the overall reaction efficiency is not provided and state-specific data were not obtained. CID experiments by Larsen and Ridge[4c] indicate that a loosely bound complex of Fe^+ with methane is the lowest energy form for $FeCH_4^+$; that such a complex with ethane may be the lowest energy form for $FeC_2H_6^+$; and that even in the propane case, species like III, IV, and V are not much more stable than the loosely bound complex. Unfortunately, these experiments are not conclusive either since the lowest energy isomer of the ion may not be the isomer that is dissociated. This situation can occur if the production of the isomeric ion is under kinetic control and there are appreciable barriers between different isomers.

Further thermochemical information regarding these intermediates can be estimated by making simple assumptions. One extreme is that $D°(Fe^+–R) \approx D°(Fe^+–CH_3) = 58 \pm 3$ kcal/mol for all alkyl groups R and that bond additivity is valid, i.e., $D°(RFe^+–H) \approx D°(Fe^+–H) = 50 \pm 2$ kcal/mol. These lead to $D°[Fe^+–(H)(R)] \approx 108 \pm 4$ kcal/mol and $D°[Fe^+–(CH_3)(R)] \approx 116 \pm 5$ kcal/mol. As noted above, however, the methyl bond energy is believed to be stronger than the H atom bond energy (by 8 kcal/mol) due to polarizability effects. If there are two polarizable ligands (such as CH_3 and R), these effects should be reduced. This reduction could be as much as 8 kcal/mol such that $D°[Fe^+–(CH_3)(R)] \approx 108 \pm 5$ kcal/mol. According to either of these estimates, oxidative addition of any C–H or C–C bond in ethane and propane is exothermic, while for methane, oxidative addition is near thermoneutral (Table II). This appears to be inconsistent with the results of Larsen and Ridge.[4c]

Since the covalent bond strengths depend on the electronic structure of the metal ion, bond additivity may be an overly simplistic assumption for estimating quantitative values for the second covalent bonds of Fe^+. For example, while the second covalent bonds to Sc^+ and V^+ are similar in strength to the first bonds,[10,22] the second methyl bond to Zn^+ is 43 kcal/mol weaker than the first.[14] Bond additivity breaks down for Zn^+ because the $4s3d^{10}$ electron configuration of Zn^+ permits formation of only one strong covalent bond. Formation of a second covalent bond to Zn^+ requires disruption of the filled 3d orbitals.

We can refine this simple bond additivity assumption by explicitly accounting for the exchange energy lost when the covalent metal ligand bonds are formed.[45] We assume that the first covalent bond to the metal ion uses a 4s orbital and the second bond uses a 3d orbital, which leaves four nonbonding 3d orbitals. For Sc^+ and V^+, this method also predicts similar first and second bond energies.[10,22] For Zn^+, it correctly predicts a strong first bond and weak second bond. For Fe^+, which has 7 electrons, the exchange energy lost upon decoupling the 4s electron from the 3d electrons is 10 kcal/mol.[46] The exchange energy lost upon

(43) Halle, L. F.; Klein, F. S.; Beauchamp, J. L. *J. Am. Chem. Soc.* **1984**, *106*, 2543–2549.

(44) Burnier, R. C.; Byrd, G. D.; Freiser, B. S. *J. Am. Chem. Soc.* **1981**, *103*, 4360–4367.

(45) Tolbert, M. A.; Beauchamp, J. L. *J. Am. Chem. Soc.* **1986**, *108*, 7509–7517.

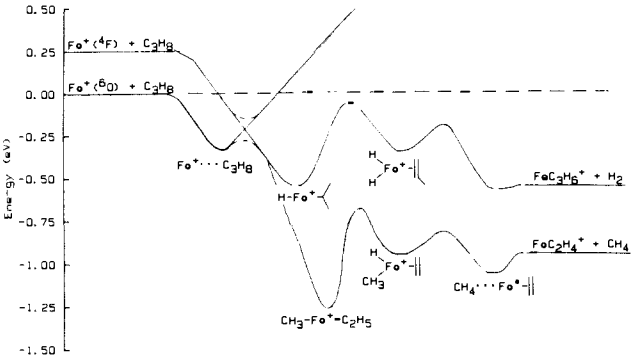

Figure 11. Semiquantitative potential energy surface for reactions 19 and 20. Diabatic surfaces are shown as solid lines. Adiabatic surfaces are shown as dashed lines. The relative thermochemistry is derived from the arguments presented in the text.

decoupling one of the 3d electrons from the remaining nonbonding 3d electrons is about 28 kcal/mol.[47] Thus, the second bond to Fe^+ can be expected to be 18 kcal/mol weaker than the first one. According to this approximation, the sum of the bond energies in $HFeR^+$ is 90 kcal/mol, *less* than any of the C–H bond energies in the alkanes studied here. For the $Fe^+(^4F)$ state (which provides 7 kcal/mol more energy), oxidative addition of a secondary C–H bond to Fe^+ is thermoneutral. The sum of the bond energies in $RFeCH_3^+$ is 98 kcal/mol, *stronger* than the C–C bonds of ethane (90 kcal/mol) or propane (88 kcal/mol). If this sum is reduced by 8 kcal/mol due to the polarizability effect discussed above, insertion into C–C bonds would be near thermoneutral. These estimates appear to be more in keeping with the results of Larsen and Ridge, but they are not consistent with the decarbonylation reaction observed by Freiser and co-workers.

One important property of these intermediates which has not been taken into consideration previously is their spin states. If Fe^+ forms two covalent σ bonds to H atoms or alkyl groups, then there remain five nonbonding electrons that reside in four nonbonding 3d orbitals on the metal. Therefore, intermediates III, IV, and V will have quartet spin ground states. Similar considerations show that intermediates like VI and VII in Scheme I will also have quartet spin ground states if the metal–alkene bond is dative.

These considerations lead to the qualitative PESs shown in Figure 11. Because the intermediate V has a quartet ground state, it is accessed *diabatically* (i.e., pertaining to a single electron configuration) by the $Fe^+(^4F)$ reactant. This correlation is consistent with the molecular orbital ideas discussed for the H_2 reaction. In the case of $Fe^+(^6D)$, the 4s electron of the ion correlates diabatically with an antibonding orbital leading to a more repulsive interaction. Thus, $Fe^+(^6D)$ is expected to diabatically correlate to a repulsive sextet surface.

Fe^+ + Methane. Methane is the alkane most similar to hydrogen not only for its small size and high symmetry but also in its C–H bond strength which is nearly the same as $D°(H_2)$. On the basis of these similarities as well as the MO and spin arguments, we might expect the mechanisms for the state-specific reactions of Fe^+ with methane and with dihydrogen to be similar. Neither $Fe^+(^4F)$ nor $Fe^+(^6D)$ reacts via insertion with H_2. Several observations suggest that Fe^+ does not insert into methane either. For example, if Fe^+ inserted into methane, we might expect to see $FeCH_2^+$ produced from process 25. Such a process is en-

$$Fe^+ + CH_4 \rightarrow FeCH_2^+ + H_2 \qquad (25)$$

dothermic by 1.22 ± 0.22 eV, ~1 eV less than reactions 6 and 7, and yet it is not seen. HAB based their conclusion that $Fe^+(SI)$ does not insert into methane on this observation.[7b] Jacobson and Freiser[48] were unable to observe the reverse of reaction 25 at thermal energies using FTICR, which implies that there is a barrier of some sort to the forward reaction as well. Scandium,[49] titanium,[13] and vanadium[10b] ions, on the other hand, do react with methane to produce these metal–methylidene ions, and they are believed to insert into H_2 as well.

Additional evidence in support of a direct mechanism for the reaction of Fe^+ and CH_4 comes from the $FeH^+/FeCH_3^+$ branching ratio of ~40:1 observed for $Fe^+(SI)$. This large branching ratio occurs even though the thermodynamic threshold for production of $FeCH_3^+$ is 0.33 eV lower than that for FeH^+. In contrast, the MH^+/MCH_3^+ branching ratio is much less for early-transition-metal ions: ~9:1 for Sc^+,[49] ~7:1 for $Ti^+(^4F)$,[13] and ~4:1 for $V^+(^5D)$.[10b] We have previously discussed simple models that quantify the branching ratio between MH^+ and MCH_3^+ production in the reactions of atomic metal ions and methane.[10b] These indicate that for a statistically behaved intermediate, a branching ratio between 4 and 20 can be expected, depending on the unknown molecular constants of MCH_3^+. A branching ratio of >20 implies a direct reaction and in the impulsive limit can be as high as 90.[50] Thus, the reaction of $Fe^+(^4F)$ with methane probably occurs via a direct mechanism and is distinct from the insertive mechanism of the early transition metals.

Even though a branching ratio for FeH^+ and $FeCH_3^+$ cannot be derived for $Fe^+(^6D)$ (since the cross section for reaction 7 is below our detectability limit), it is nonetheless clear that $Fe^+(^6D)$ does not insert into methane. For reaction 6, the cross section for $Fe^+(^6D)$ has both the threshold and the peak shifted to higher energy compared with that for $Fe^+(^4F)$. Furthermore, the reaction efficiency is 20 times less for $Fe^+(^6D)$ than for $Fe^+(^4F)$ when compared at their maxima. This behavior is typical of an impulsive reaction,[1,11c] where the ion interacts primarily with the hydrogen atom it removes, either by stripping or by collision along the $H–CH_3$ bond axis. In either case, the ion will be particularly sensitive to the orientation of the methane molecule resulting in a small cross section.

In conclusion, it is clear that $Fe^+(^6D)$ reacts with methane much as it does with dihydrogen, via an impulsive direct mechanism. From our data it seems probable that reaction of $Fe^+(^4F)$ and methane proceeds through a direct mechanism, also as observed for reaction with dihydrogen. These mechanisms are consistent with the thermochemistry of a $HFeCH_3^+$ intermediate which is estimated to be bound by no more than 3 ± 4 kcal/mol and could lie as high as 15 kcal/mol above ground-state reactants, 8 kcal/mol above $Fe^+(^4F) + CH_4$.

Fe^+ + Ethane. The endothermic reaction channels of ethane with Fe^+ (reactions 8–10) lend themselves straightforwardly to the kind of analysis presented for reactions with methane. In all of them, $Fe^+(^6D)$ reactions show slow onsets, delayed peaks, and lower reactivity relative to $Fe^+(^4F)$, i.e., behavior typical of an impulsive reaction.

The behavior of $Fe^+(^4F)$ is not resolved so easily. First, we observe a ratio of about 70:1 for FeH^+ versus $FeC_2H_5^+$ production, again suggesting a direct reaction. $MC_2H_5^+$ is not observed in the reaction of ethane with Sc^+,[22] Ti^+,[49b] or V^+,[10a] however, indicating that factors other than reaction dynamics probably control this ratio. Second, if $Fe^+(^4F)$ inserted into a C–H or C–C bond, we might anticipate observing the production of $FeCH_2^+$ by elimination of methane. This reaction *is* observed for Sc^+, Ti^+, and V^+, the metal ions on the left side of the periodic table which are believed to react with dihydrogen and methane via insertion. Since $FeCH_2^+$ is not observed at low energies, direct reaction of $Fe^+(^4F)$ and ethane may be occurring, although it is possible that CH_4 elimination from $Fe(CH_3)_2^+$ has a substantial barrier in excess of the endothermicity. Barriers of 0.5 to 1.0 eV are known to exist in the Sc^+,[22] Ti^+,[49b] and V^+ [10a] systems for this process.

(46) Schilling, J. B.; Goddard, W. A., III; Beauchamp, J. L. *J. Am. Chem. Soc.* **1986**, *108*, 582.
(47) Schilling, J. B.; Goddard, W. A., III; Beauchamp, J. L., unpublished results.
(48) Jacobson, D. B.; Freiser, B. S. *J. Am. Chem. Soc.* **1985**, *107*, 4373–4379.
(49) (a) Armentrout, P. B. In *Structure/Reactivity and Thermochemistry of Ions*; Ausloos, P., Lias, S. G., Eds.; D. Reidel: Dordrecht, 1987; pp 97–164. (b) Sunderlin, L. S.; Armentrout, P. B., work in progress.
(50) See ref 10b for a full discussion of the problem.

Third, if $Fe^+(^4F)$ does react to form an $H-Fe^+-C_2H_5$ intermediate, then the dehydrogenation reaction is easily explained by β-hydrogen elimination. Further, the existence of such an intermediate would explain the coupling noted between the $FeC_2H_4^+$ and FeH^+ channels. These observations are not easily accounted for by a direct mechanism.

Overall, we cannot rule out either insertion or a direct mechanism for the $Fe^+(^4F)$ + ethane reaction. It is likely that both mechanisms occur but at different kinetic energies. At low energies, it appears that oxidative addition to form an $HFeC_2H_5^+$ intermediate is probably occurring, but very inefficiently. This is consistent with the thermochemistry of such an intermediate as estimated above, between -8 ± 4 and $+10$ kcal/mol. At higher energies, more direct mechanisms seem to be responsible for the bulk of the observed reactivity.

Fe^+ + Propane: Endothermic Reactions. As with ethane, the endothermic reactions of $Fe^+(^6D)$ with propane are consistent with an impulsive reaction mechanism. The reactivity at threshold, however, is somewhat greater here than for the smaller systems. This increase could imply that the sextet surface is less repulsive for propane than for the smaller systems, presumably because the decreasing symmetry makes the reactivity rules outlined by Elkind and Armentrout[11,12,17] less rigorously obeyed.

Once again, determining the mechanism for reaction of $Fe^+(^4F)$ is more difficult. As in the methane and ethane systems, the branching ratio between FeH^+ and FeR^+ provides some information although here no $FeC_3H_7^+$ is observed directly. As discussed above, however, any $FeC_3H_7^+$ formed may decompose to $FeC_3H_5^+$ via reaction 18a, which would mean that the ratio $FeH^+/FeC_3H_7^+ \leq FeH^+/FeC_3H_5^+ \approx 200$. This large ratio implies a direct mechanism but is not unambigurous evidence, as discussed above for the analogous reaction in the ethane system. Another pertinent observation is the rapid decline of the exothermic reaction channels for $Fe^+(^4F)$ when the endothermic channels become thermodynamically available. As discussed above, such coupling implies that these channels share common reaction intermediates, presumably III, IV, and V of Scheme I. We conclude that while direct reactions may contribute to the reactivity at high kinetic energies, the endothermic reactions apparently have the same intermediates as the exothermic channels.

Although it becomes more difficult to definitively determine state-specific reaction mechanisms for larger systems, the behavior of reactions 12 and 13 shows that the MO arguments outlined above are still valid here. For $Fe^+(^4F)$, reaction 12 is about three times as efficient as reaction 13, while for $Fe^+(^6D)$, it is roughly 15 times more efficient. As noted above, the factor of 3 is a result of the site preference for H atom versus H^- transfer. For the ^6D state, however, H^- transfer is clearly much less favorable. In order to form FeH, Fe^+ must accept a pair of 1s electrons in its 4s orbital. Since $Fe^+(^4F,3d^7)$ has an empty 4s orbital, it can do so easily; but for $Fe^+(^6D,4s3d^6)$, the acceptor orbital is occupied such that H^- transfer is disfavored.

Fe^+ + Propane: Exothermic Reactions. Oxidative addition of a C–C or a C–H bond (Fe^+ insertion) as in Scheme I appears to be the most reasonable mechanism for producing the products of exothermic reactions 19 and 20. Indeed, the thermochemical estimates discussed above suggest that intermediates III, IV, and V (with stabilities of -11 to 7 kcal/mol, -8 to 10 kcal/mol, and -28 to -2 kcal/mol, respectively) are more stable than their counterparts in the methane and ethane systems. Further, the lack of low-energy scrambling implies that once VI and VII are formed they rarely return to III, IV, or V, i.e., H_2 and CH_4 elimination is fast. This could be because the barriers between these intermediates are larger than those leading to product formation or because of frequency factor differences in the isomerization and elimination processes. This conclusion contrasts with the situation that must exist for species I and II which have been observed to scramble by Halle et al.[43] Apparently, the additional H or alkyl group is sufficient to change the energy necessary for a β-group shift. This seems reasonable since the extra ligand should have both steric and electronic effects on the rearrangement process.

Scheme I

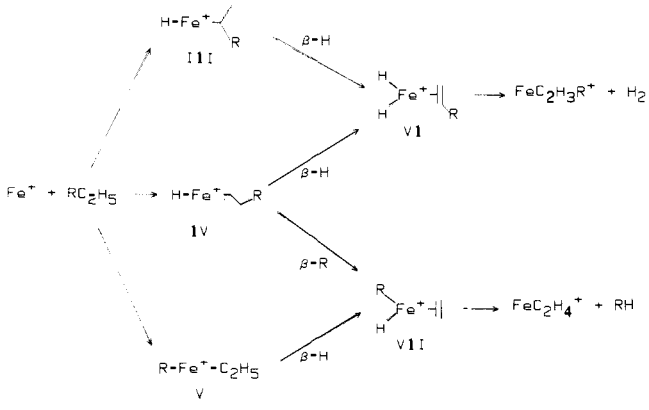

An alternative mechanism for the exothermic reactions is that full insertion to form two covalent Fe–R bonds does not occur but rather a partial charge-transfer complex, $C_3H_8^{+\delta}-Fe^{+\delta}$, is formed. This intermediate could then decompose in a fashion characteristic of an isolated alkane ion. However, $C_3H_8^+$ does not lose H_2 efficiently[51] in contrast to the observation here of reaction 19. Also the behavior of this type of intermediate should be relatively independent of the electronic state of the Fe^+. This demonstrates that the Fe center plays an active role in the reactions.

Another feature of the exothermic reactions which needs to be explained is the branching ratio between reactions 19 and 20. It is 1:3, *independent* of ion kinetic energy *and* electronic state. Previous researchers[4c,43,52] have commented that the exothermic reactions of Fe^+ and alkanes show roughly the same branching ratio behavior regardless of how the ions are produced. They made the reasonable assumption that this indicates that these reactions are dominated by one electronic state.[4c,7c,43,52] The present results demonstrate that this conclusion is fallacious.

The underlying reasons behind this unexpected behavior are not entirely obvious although the branching between the two products must occur at some point along the reaction coordinate which is insensitive to translational and electronic energy. We can imagine several possible explanations for the independence from translational energy. (1) If H_2 loss occurs via C–H bond activation while CH_4 loss occurs via C–C bond activation, then the product branching ratio will be determined by the ratio of C–H to C–C bond insertion. If this ratio depends primarily on the orientation of the molecule as the ion approaches, it may be relatively insensitive to the kinetic energy even though C–C activation is expected to be $\sim$19 kcal/mol more exothermic than C–H bond activation and the C–C bond is less accessible. (2) Reaction 20 could occur exclusively via primary C–H bond activation to form IV followed by β-methyl transfer and methane elimination, rather than via C–C bond activation to form V (Scheme I).[53] Then the competition between reactions 19 and 20 would involve oxidative addition of C–H bonds that are equally accessible and differ in strength by <3 kcal/mol (Table II). The branching ratio would then be determined primarily by the 3:1 ratio of primary to secondary C–H bonds. Despite being thermodynamically favored, C–C bond insertion may be disfavored due to steric restrictions, a result more in keeping with solution-phase studies. On the other hand, the weaker C–C bond presumably makes β-methyl transfer much more facile than β-hydride transfer for intermediate IV. Since 1,3-dehydrogenation is seen, some γ-hydrogen transfer from IV also must be occurring although inefficiently ($\sim$5% of the $FeC_2H_4^+$ channel). Unfortunately, labeling studies cannot definitively determine the insertion site, as earlier researchers have pointed out.[3] (3) Another potentially influential factor for the branching ratio is angular momentum

(51) Stockbauer, R.; Inghram, M. G. *J. Chem. Phys.* **1976**, *65*, 4081–4092.
(52) Reents, W. D., Jr.; Strobel, F.; Freas, R. B., III; Wronka, J.; Ridge, D. P. *J. Phys. Chem.* **1985**, *89*, 5666–5670.
(53) Schultz, R. H.; Armentrout, P. B. *J. Phys. Chem.* **1987**, *91*, 4433–4435.

conservation. We have discussed this problem for exothermic reactions previously.[9] Qualitatively, this effect will tend to favor reaction 20 over reaction 19. No reliable quantitative estimate can be made because of the uncertainties in the rotational and translational excitation of both sets of products.[54] Angular momentum conservation cannot be the only factor determining the branching ratio, however, because if it were, H_2 and CH_4 elimination would have to occur from the same intermediate, which seems very unlikely.

The branching ratio is also independent of electronic state. This effect is easily understood if the point(s) on the PES where the branching is determined is *exactly the same for both states*.[56] If so, the quartet and sextet surfaces shown in Figure 11 must mix and the branching point occurs after the crossing between these surfaces. Such a surface interaction also may explain the differences observed between $Fe^+(^6D)$ and $Fe^+(^4F)$ in the cross sections for reactions 11, 19, and 20 (Figures 5 and 10). This idea is explored further in the next section.

Nonadiabatic Behavior

Fe^+ + Propane. The most unusual aspect of the reaction of Fe^+ and small alkanes is the marked difference in the behavior between the ^6D and ^4F states in the exothermic channels. This study marks the first time that this kind of state-dependent behavior has been seen. We find these data are best explained by the crossing between the quartet and sextet PESs, illustrated qualitatively in Figure 11. This can occur because at low kinetic energies, $Fe^+(^6D)$ behaves *adiabatically*, i.e., the surface crossing is avoided, although not completely, since $Fe^+(^4F)$ also reacts at low energy. At low kinetic energies, the nuclei are moving slowly relative to the electrons, and the Born–Oppenheimer (B–O) approximation is valid. Then spin–orbit coupling is likely to be efficient such that an avoided surface crossing results, presumably for surfaces having the same values of J. This conservation requirement is not very restrictive, however, since both states of Fe^+ have similar ranges of J values: $J = 9/2$ to $1/2$ for $Fe^+(^6D)$ and $J = 9/2$ to $3/2$ for $Fe^+(^4F)$. As the kinetic energy of the nuclei increases, the B–O approximation breaks down, and diabatic correlation (of $Fe^+(^4F)$ to product and $Fe^+(^6D)$ to a repulsive surface) becomes increasingly dominant. Consequently, the reactivity of $Fe^+(^6D)$ declines faster than predicted by eq 2 while that for $Fe^+(^4F)$ actually increases (Figure 10). Thus, *the cross section behavior above 0.5 eV in the exothermic channels and in all the endothermic channels is nonadiabatic.*

As we have discussed earlier,[53] the simplest approach to understanding nonadiabatic behavior is the Landau–Zener theory.[57] This model treats the collisions of two atoms which are moving with relative velocity v along a PES. The probability of making the crossing between adiabatic surfaces (staying on the diabatic surfaces) on a single pass is $p = \exp(-A/v)$, where A is the coupling strength between the two surfaces or, equivalently, $p \propto \exp[-(E_c)^{-1/2}]$, where E_c is the relative kinetic energy at the crossing. E_c depends on both the kinetic energy of the reactants and the potential energy at the crossing point. Since the potential is one-dimensional, the reactants can pass the crossing seam twice, once as they approach and once as they separate. Therefore, the nonadiabatic probability, $P = 2p(1-p)$, has a maximum value of $1/2$ and can never be greater than the adiabatic probability, $(1-P)$. Although the theory clearly does predict a kinetic energy-dependent competition between adiabatic and nonadiabatic channels, it cannot quantitatively account for the observed state-specific behavior.[58]

The failure of the Landau–Zener model in its application to the present system is not surprising considering its simplicity. Nevertheless, understanding the reasons behind its failure are instructive. The model assumes that two structureless particles interact on two PESs. Here, we have 58 reactant PESs (28 from $Fe^+(^4F)$ and 30 from $Fe^+(^6D)$). In addition, there are 30 internal degrees of freedom in the present system. This means that the reactants could pass through the crossing seam only once (immediately forming III, IV, or V and then going on to products); or many times (the reactants remain in the ion-induced dipole well of the ground-state adiabatic surface or the potential well on the excited-state adiabatic surface for many rotational periods); or not at all (the reactants form these initial complexes but decompose back to reactants before reaching the surface crossing). Furthermore, the differences in the 3d orbital populations mean that not all of the quartet surfaces are equally attractive nor are all of the sextet surfaces equally repulsive. There must therefore be many surface crossings at different potential energies and geometries. Finally, the maximum reaction efficiency, given by the sum of the ^6D and ^4F cross sections, is only 22% (+10%, −7%) of the collision limit, eq 2, meaning that some factor other than the surface crossing limits the reactions.

The limitation on the overall reaction efficiency cannot be thermodynamic since reactions 19 and 20 exhibit no activation barriers. It could be related to angular momentum constraints in the exit channels. Again reliable quantitative estimates of this effect rely on many assumptions, but qualitatively, this effect probably falls short of explaining the reduced reaction efficiency.[59] The low reaction efficiency could be because many of the loosely bound $Fe^+\cdots C_3H_8$ complexes never reach the critical surface crossing due to the many degrees of freedom, as suggested above. Another possibility is that III, IV, and V return to reactants more often than they rearrange to VI and VII. This conjecture is consistent with the lack of scrambling in this system. It also would provide a mechanism for quenching if $Fe^+(^4F)$ reacted to form III, IV, and V which then returned to reactants in their ground states. This is a likely (but unobservable in our instrument) reaction channel for $Fe^+(^4F)$ at low kinetic energies.

Fe^+ + Other Alkanes. This type of nonadiabatic surface mixing can also be used to explain the behavior of the cross section for reaction 11 which exhibits separate exothermic and endothermic portions for the SI beam (Figure 5). As in the propane system (Figure 11), the first interaction between Fe^+ and ethane will be attractive due to the ion–induced dipole potential. Since C_2H_6 ($\alpha = 4.4$ Å^3) is only 70% as polarizable as C_3H_8 ($\alpha = 6.2$ Å^3),[55] this polarization well will be shallower for ethane. Further, the $H–Fe^+–C_2H_5$ insertion intermediate is thermodynamically less stable than the intermediates in the propane system. These two effects cause the surface crossing to occur earlier along the reaction coordinate and therefore at a higher potential energy. Thus, at a given kinetic energy, access to the insertion intermediate will be thermodynamically less favorable here than for propane, and dehydrogenation should be much less efficient. At higher kinetic energies, the diabatic behavior again becomes more likely such that $Fe^+(^4F)$ shows an apparently endothermic dehydrogenation reaction. This is well separated in energy from the inefficient exothermic dehydrogenation by $Fe^+(^6D)$.

For larger alkanes, the polarization wells become deeper such that the crossing should occur at still lower potential energies. Mixing of the diabatic surfaces should then be more efficient,

(54) A quantitative estimate can be made if rotational excitation of the products is ignored. Then the appendix in ref 9 outlines arguments that lead to the prediction that $\sigma''(20)/\sigma'(19) = (\alpha''E''/\alpha'E')^{1/2}\mu''/\mu'$ where α is the polarizability of the neutral product ($\alpha'(H_2) = 0.8$ Å^3 and $\alpha''(CH_4) = 2.56$ Å^3),[55] μ is the reduced mass of the products ($\mu' = 2.0$ amu and $\mu'' = 13.4$ amu), and E' and E'' are the kinetic energies of the products for reactions 19 and 20, respectively. If E' and E'' are comparable, then $\sigma''/\sigma' = 12$.

(55) Rothe, E. W.; Bernstein, R. B. *J. Chem. Phys.* **1959**, *31*, 1619–1627.

(56) It is interesting to note that Reents et al. (ref 52) made a similar suggestion for Fe^+ reactions based on their studies of Cr^+ reactivity and quenching.

(57) Landau, L. D. *Phys. Z. Sowjetunion* **1932**, *2*, 46. Zener, C. *Proc. R. Soc.* A **1932**, *137*, 696. Stueckelberg, E. C. G. *Helv. Phys. Acta* **1932**, *5*, 369.

(58) Modeling of the cross sections was attempted by assuming that the reactants could pass through the crossing region once, twice, or three times. These probabilities were compared with the relative probabilities for both Fe^+ states and to the absolute cross sections by including the collision cross section, eq 2.

(59) For example, if rotational excitation of the products is ignored, arguments detailed in ref 9 predict that the maximum cross section for reaction 20 is given by $0.35\sigma_{LGS}(1 + \Delta H/E)^{1/2}$, where ΔH is the exothermicity of the reaction, ~0.8 eV. This exceeds σ_{LGS} at kinetic energies below 0.12 eV, and even at 1 eV, the predicted cross section is $\sigma_{LGS}/2$.

leading to high reactivity for $Fe^+(^6D)$ at low kinetic energies in these systems. Indeed, ICR and FTICR studies show that larger alkanes do react with Fe^+ in efficient exothermic reactions.[3-5]

Finally, how do we reconcile the behavior observed here for the exothermic reactions with the ideas developed for understanding the reactions of transition-metal ions with dihydrogen? The reactivity "rules" originally suggested by Elkind and Armentrout[11,12,17] for H_2 reactions are *diabatic* rules. The present observations illustrate that they break down when there is sufficient spin–orbit coupling to allow reactants to follow the adiabatic PESs.

Summary

We present a detailed study of the reactions of Fe^+ with methane, ethane, and propane. The populations of Fe^+ electronic states are manipulated by using different ion sources. Analysis of the data yields the state-specific behavior of the ^6D ground and ^4F first excited states of Fe^+. From the state-resolved behavior of the ions, we can deduce a wealth of information about the reaction thermochemistry and dynamics of these systems.

The threshold behavior of the endothermic channels enables us to determine values for Fe–H, Fe^+–H, Fe^+–CH_3, and Fe^+–C_2H_5 bond strengths. The bond strengths reported here for the cationic species differ by about 10 kcal/mol from previous determinations.[7] The differences lie primarily in our ability to determine the state-specific reactivity. In all cases, we find that it is the first excited state of the ion that dominates the observed reactivity at the observed threshold.

The ground state is much less reactive than the first excited state in all endothermic reactions studied here despite being only 0.25 eV lower in energy. In this respect, the behavior of Fe^+ with small alkanes is much like its behavior with hydrogen. The enhanced reactivity of the first excited state is easily rationalized by simple molecular orbital arguments. These arguments predict, and the data confirm, that the ground state ion will react via an inefficient impulsive process. For reaction with CH_4, as with H_2, the first excited state appears to react via a direct mechanism. For the larger alkanes, insertive intermediates appear to be thermodynamically allowed. The products observed are most easily explained via such a mechanism at low energy, although it appears that more direct mechanisms may be involved at higher kinetic energies. Overall, *the electronic considerations for C–H and C–C bond activation appear to be directly analogous with those discussed previously for H–H activation.*[12]

For exothermic reactions of Fe^+ with ethane and propane, it is the ground state that is more reactive at low energies. At higher energies, the first excited state is once again more reactive. This difference in behavior is attributed to a crossing of quartet and sextet surfaces which is avoided due to spin–orbit mixing at low kinetic energy but permitted at higher energy. Simple theories such as the Landau–Zener formalism are unable to quantitatively account for the behavior of the system. Finally, the branching ratio between the two exothermic reactions of Fe^+ and propane is independent of electronic and kinetic energy. This shows that the branching point occurs after the surface crossing.

The type of surface crossing evident in the present study should be a common feature of ionic and neutral transition-metal systems, due to the large number of electronic states that are generally involved. Indeed, such surface interactions have been postulated in a number of other systems.[6,10,13,22,52] The present results provide hope that quantitative information concerning these spin–orbit interactions can be obtained.

Acknowledgment. This work was supported by National Science Foundation Grant No. CHE-8608847.

Neutral Square Planar Cobalt(III) Complexes

John C. Brewer, Terrence J. Collins,*[1] Milton R. Smith, and Bernard D. Santarsiero

Contribution No. 7524 from The Chemical Laboratories, California Institute of Technology, Pasadena, California 91125. *Received February 19, 1986*

Abstract: The monoanionic square planar cobalt(III) complex, $[PPh_4][Co(\eta^4\text{-HMPA-DMP})]$ (**4**) (H_4HMPA-DMP = 2,4-bis(2-hydroxy-2-methylpropanamido)-2,4-dimethyl-3-oxopentane), has been prepared and characterized by ^1H NMR, solid state and solution magnetic properties, X-ray crystallography, and IR spectroscopy. Compound **4**, and related anionic square planar cobalt(III) complexes, can be alkylated at an amido-*N* oxygen atom to afford the first examples of neutral square planar cobalt(III) complexes. These species have been characterized by ^1H NMR, solid-state magnetic properties, mass spectroscopy and elemental analysis, a solution molecular weight determination, and IR spectroscopy. All of the compounds exhibit well-resolved paramagnetically shifted ^1H NMR spectra. Depending upon the donor properties, certain PAC ligands afford stable octahedral cobalt(III) complexes whereas others produce the coordinatively unsaturated square planar complexes. This is of potential significance in the search for new inorganic reagents for atom-transfer and inner-sphere oxidations.

The incompatibility of the majority of the ligands of homogeneous inorganic chemistry with strongly oxidizing media is a limitation confronting the development of selective oxidizing agents. In the past several years our attention has been focused on the design of oxidation resistant ligands. We have shown that it is possible to prepare strongly oxidizing, solution stable complexes by identifying building blocks for polyanionic chelating (PAC) ligands that are compatible with strongly oxidizing media.[2] In the course of this work we have discovered ligand complements that convey unusual chemical and physical properties to metal complexes such as the formation of nonplanar amido-*N* ligands and have identified causative structural and bonding features.[3]

One significant property-determining feature of a ligand complement is the donor capacity, i.e., the ability of a ligand complement to transfer electron density to a metal center in a given oxidation state relative to all other ligand complements of the same topology. An important effect of changing ligand donor capacities can be illustrated by an unusual feature of the coordination chemistry of cobalt(III). The vast majority of cobalt(III) complexes are octahedral. However, when the ligand complement consists of four strongly σ-donating anions the axial Lewis acidity

(1) Dreyfus Teacher–Scholar 1986–1990, Alfred P. Sloan Research Fellow 1986–1990. Present address: Department of Chemistry, Carnegie Mllon University, 4400 Fifth Street, Pittsburgh, PA 15213.

(2) (a) Anson, F. A.; Collins, T. J.; Gipson, S. L.; Keech, J. T.; Krafft, T. E.; Santarsiero, B. D.; Spies, G. H. *J. Am. Chem. Soc.* **1984**, *106*, 4460–4472. (b) Anson, F. C.; Collins, T. J.; Coots, R. J.; Gipson, S. L.; Keech, J. T.; Krafft, T. E.; Santarsiero, B. D.; Spies, G. H. *Inorg. Chem.* **1987**, *26*, 1161–1168. Anson, F. C.; Collins, T. J.; Gipson, S. L.; Keech, J. T.; Krafft, T. E. *Inorg. Chem.* **1987**, *26*, 1157–1160.

(3) (a) Anson, F. C.; Collins, T. J.; Gipson, S. L.; Keech, J. T.; Krafft, T. E.; Peake, G. T. *J. Am. Chem. Soc.* **1986**, *108*, 6593–6605. (b) Collins, T. J.; Coots, R. J.; Furutani, T. T.; Keech, J. T.; Peake, G. T.; Santarsiero, B. D. *J. Am. Chem. Soc.* **1986**, *108*, 5333–5339. (c) Collins, T. J.; Lai, T.; Peake, G. T. *Inorg. Chem.* **1987**, *26*, 1674–1677.

0002-7863/88/1510-0423$01.50/0